5

Continuous Measurement: Diffusive Case

In the previous chapters, we have learned about projective measurements, generalized measurements, weak measurements, and sequences of the same. The weak value involved a weak measurement followed by a strong one. We now introduce the concept of a continuous measurement by considering a sequence of many weak measurements, one after the other, not bothering to reset the system back to the same initial condition. This weak measurement sequence has results $r_1, r_2, \ldots r_N$, where r_j can be either continuous or discrete. We consider a timeline, discretized into equally spaced time chunks of size Δt, so that after N measurements, a total time $T = N\Delta t$ has elapsed. We consider the limit where the measurement progressively weakens as $\Delta t \to 0$, to get a well-defined mathematical limit.

Continuous quantum measurements were developed by a number of scientists coming at the problem from different perspectives, including Balavkin, Barchielli, Carmichael, Milburn, Wiseman, Diósi, and Gisin, starting in the mid 1980s. Depending on the type of detectors involved, one can realize different types of continuous quantum measurements. In this chapter we focus on the diffusive quantum trajectories, while in the next chapter we focus on quantum jump continuous measurements.

Each measurement j is associated with a measurement operator $\hat{\Omega}_j$, so starting with a well-defined state $|\psi_0\rangle$, we define a quantum map from each time to the next,

$$|\psi_j\rangle = \frac{\hat{\Omega}_j|\psi_{j-1}\rangle}{||\hat{\Omega}_j|\psi_{j-1}\rangle||}, \tag{5.1}$$

where $j = 1, \ldots, N$. This creates a chain of states, dependent on the initial state and all subsequent measurements. The strength of the measurement can be controlled by Δt, so as $\Delta t \to 0$, the sequence of states can become a diffusive process in the Hilbert space. Importantly, this is not the only option: another class of quantum trajectories is called quantum jumps and will be discussed in the next chapter.

https://doi.org/10.1017/9781009103909.006 Published online by Cambridge University Press

The sequence of measurement results $\{r_j\}$ is called a *measurement record*, and the sequence of quantum states $\{|\psi_j\rangle\}$ is called a *quantum trajectory*.

Rather than launch into the abstract, mathematical description of this physics, we begin with motivating physical experiments: an electron in a double-quantum-dot being measured with a quantum point contact, and a superconducting circuit being dispersively measured by microwave frequency electromagnetic radiation.

5.1 Measuring the Location of an Electron on a Double Quantum Dot with a Quantum Point Contact

We consider a first experiment involving condensed matter physics. In a two-dimensional electron gas, formed by a layered semiconductor material that confines electron motion to a plane, metallic top-gates further constrict electron motion with electrical potential control. These metallic gates can cause islands of electrons to form in small regions, called *quantum dots*. If they are small enough, they become a kind of artificial atom because the energy of the electrons is quantized, as a result of being in a confining potential.

We can complicate this picture by considering a double quantum dot, where we imagine two potential well bowls close together, making a kind of dumbbell (see Fig. 5.1). In this geometry, we consider the simplest case of a single electron, which can be localized on the left side of the double quantum dot (DQD), or on the right side. Taken in isolation, these dots have their own energy levels, but the possibility of the electron tunneling from left or right or vice versa results in a hybridization of the energy levels. If we denote $|L\rangle$ and $|R\rangle$ as the states of an electron confined to the ground state of either the left or the right well, and the wells are symmetric, then $|\psi_\pm\rangle = (|L\rangle \pm |R\rangle)/\sqrt{2}$ describes the ground and first excited states, respectively. In Exercise 5.6.1 you will prove this statement.

If we suppose the electron is localized in the left well (for example), then the tunneling process will cause flopping back and forth between wells, described by the state

$$|\psi(t)\rangle = \cos(\Delta t/\hbar)|L\rangle - i\sin(\Delta t/\hbar)|R\rangle. \tag{5.2}$$

More generally, if we suppose the potential double well is slightly tipped, so the difference between the left and right wells' energy is ϵ, this situation can be modeled within the two-state approximation by adding a term $\epsilon\hat{\sigma}_z/2$ to the Hamiltonian, so the more general two-state system Hamiltonian is given by

$$H = \frac{\epsilon}{2}\hat{\sigma}_z + \frac{\Delta'}{2}\hat{\sigma}_x. \tag{5.3}$$

https://doi.org/10.1017/9781009103909.006 Published online by Cambridge University Press

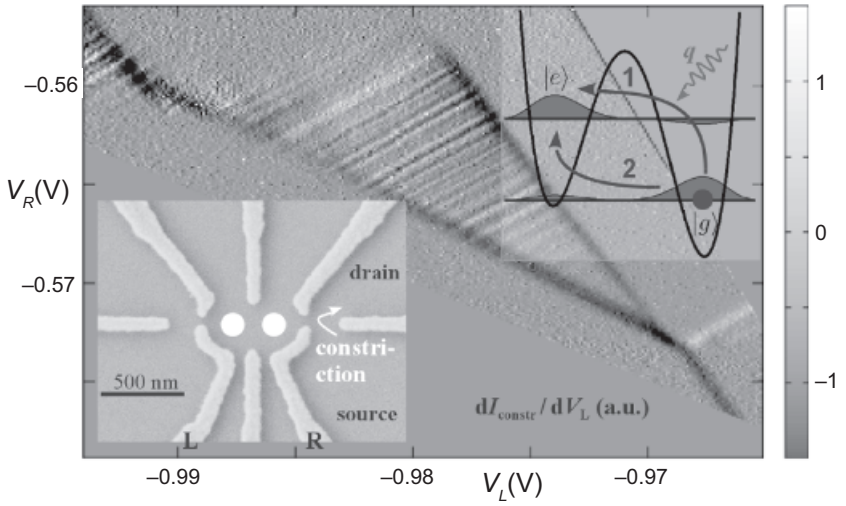

Figure 5.1 A double quantum dot with a quantum point contact charge sensor is shown in the scanning electron micrograph in the lower left. The light grey structures are metal electrodes used to gate an AlGaAs/GaAs heterostructure with a two-dimensional electron system 80 nm beneath the surface. The main plot shows the transconductance, measured at 30 mK, of the quantum point contact sensor in response to a small modulation of the left electrode voltage. This response is then plotted over a range of bias voltages applied to the left and right gates. The bright/dark lines correspond to single-electron transitions (Granger et al., 2012). The stripes are attributed to an interference pattern between two different paths for single-phonon absorption which create a nonequilibrium population of the excited state, illustrated in the upper right. Adapted with permission from Springer Nature and Stefan Ludwig.

Here we have substituted $\Delta = \Delta'/2$ for a symmetric Hamiltonian. More generally, a $\hat{\sigma}_y$ could be added, but a basis transformation can always align the operator along one transformed transverse axis.

How can such a system be measured? Note that the electron has an electric charge on it. This physical property can be used to determine where it is. We must therefore design a charge detector that can rapidly and efficiently determine where the electron is located. We will employ a nearby electrical conductor to sense the presence of the nearby charge. An optimal choice turns out to be a *quantum point contact*. This device is formed using metallic top gates to further constrict electron flow to a narrow channel, similar to a river channeled through a narrow constriction. The quantum point contact (QPC) is a mesoscopic version of a resistor; we can think of the constriction as an electron-scattering barrier that the electrons must traverse if they are to cross from one side to the other. The contact is connected

https://doi.org/10.1017/9781009103909.006 Published online by Cambridge University Press

on both sides to electron reservoirs, so an applied electrical bias V results in the flow of electrical current I. The current obeys Ohm's law, $I = GV$, where G is the conductance of the contact. While a detailed discussion of the mesoscopic transport physics is beyond the scope of this book, we quote the Landauer–Büttiker formula for transport (Büttiker, 1986), that relates conductance to transmission,

$$G = \frac{2e^2}{h}\mathcal{T}. \tag{5.4}$$

Here, e^2/h is the conductance quantum, the factor of 2 corresponds to two spin components, while $\mathcal{T}$ is the transmission coefficient of the scattering region. The qualitative physics behind this formula is that when an electrical bias is applied, the Fermi energy of the electrons on one side is elevated by the chemical potential. This allows fermions in filled states (at zero temperature) to find empty states on the other side of the barrier. The constriction only allows a discrete number of quantum channels to open up (corresponding to quantizing the transverse wavefunction according to the boundary condition), quantizing conductance in units of $2e^2/h$. We focus here on the case where the contact is operating between the 0 and 1 channels. The scattering transmission probability is controlled by the shape of the scattering potential, and its height in particular. If the peak of the barrier exceeds $E_F + eV$, then only tunneling processes can transport electrons across the barrier, so we have very small current, $\mathcal{T} \ll 1$. On the other hand, as the energy of the electrons is increased (or the barrier height is decreased), the transmission gradually increases, up to a fully open channel.

Now that we have described both the DQD and the QPC, we can combine them, where the DQD is viewed as the system and the QPC is viewed as the detector (see Fig. 5.2). By fabricating these (semi)conductors nearby, an effective geometric capacitance exists between them. Therefore, a single electron being either L or R on the DQD causes the QPC potential to be V_L or V_R, causing a slight difference in the constriction of the contact. This results in the electrical conductance being either G_L or G_R, which in turn causes the electrical current to be I_L or I_R, a little like Schrödinger's cat. Using this deductive chain, by measuring electrical current with an ammeter, we can measure the position of the charge on the DQD. While very sensitive, the small difference in position of the electron, together with weak coupling, results in a *weakly responding detector*, so we typically have the situation where $I_L - I_R \ll (I_L + I_R)/2$. Importantly, the detector has intrinsic and extrinsic sources of noise that must be accounted for to obtain a complete picture. This goes hand in hand with the sensitivity of the device, a topic we now examine.

The potential landscape around the QPC can be modeled as a saddle-point: there the potential rises and falls as the electrons traverse the hill, while the walls of the pass rise up on both sides. This potential takes the form $V(x, y) =$

https://doi.org/10.1017/9781009103909.006 Published online by Cambridge University Press

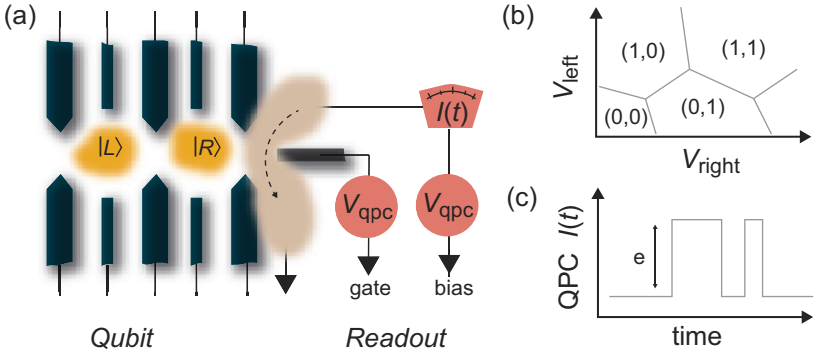

Figure 5.2 (a) A double quantum dot can be formed by arranging metallic electrodes on the surface of a semiconductor substrate doped with a 2D electron gas slightly below the surface. Applying voltages on these gates can pinch off charge-rich regions, forming dots of a variable number of electrons. High-frequency signals are coupled with select electrodes to induce quantum state transitions. (b) A typical stability diagram is shown where voltages applied via the left and right gates tune the number of electrons in each dot, expressed as a pair (left, right). A common measurement scheme involves charge sensing one or both dots though a quantum point contact placed in proximity to the quantum dot. (c) A current traveling through the narrow conductive channel of the point contact is very sensitive to single electron changes in the dot.

$V_0 - (1/2)m\omega_x^2 x^2 + (1/2)\omega_y^2 y^2$, where the electron passes in the x direction, and the walls rise up in the y direction. For this potential, a scattering problem with particles coming from the negative x direction with energy E can be solved exactly (Büttiker, 1990) to give the transmission coefficient

$$\mathcal{T} = \frac{1}{1+e^{-\epsilon}}, \qquad \epsilon = \frac{2\pi}{\hbar\omega_x}\left(E - V_0 - \frac{\hbar\omega_y}{2}\right). \tag{5.5}$$

Here we see that if the electron's energy is below the top of the energy barrier V_0, the transmission becomes very small, while if the electron's energy is well above V_0, then the transmission limits to 1, indicating an open channel. The conductance takes into account electrons traversing the barrier over a range of energies, but if the applied voltage is small compared to the Fermi energy, $eV \ll E_F$, we can approximate all transport as taking place at the Fermi level, so the conductance is given by (5.4), where the electron's energy is taken at the Fermi energy, $E = E_F$.

The electron position on the DQD controls the potential energy V_0 of the QPC potential. Thus, the place of maximum sensitivity for the detector corresponds to the point of maximum slope,

$$\frac{\partial I}{\partial V_0} = \frac{2e^2V}{h}\frac{\partial \mathcal{T}}{\partial \epsilon}\frac{\partial \epsilon}{\partial V_0} = -\frac{2e^2V}{h}\frac{2\pi}{\hbar\omega_x}\frac{e^{-\epsilon}}{(1+e^{-\epsilon})^2}. \tag{5.6}$$

https://doi.org/10.1017/9781009103909.006 Published online by Cambridge University Press

From this expression, we can see the slope is maximized in magnitude when $\epsilon = 0$, or $\mathcal{T} = 1/2$.

To fully understand the detector physics, we must also understand the noise. Detector noise can come from many places: there is thermal noise (also called Johnson–Nyquist noise) that is present in all dissipative devices, there is $1/f$ noise at low frequency, electronic flicker and telegraph noise, and so on. Here we focus on a fundamental source of noise intrinsic to the detection process – shot noise of the electrons. So long as $eV \gg k_B\Theta$, the thermal energy, we can neglect the thermal noise contribution, where Θ is the temperature. Electronic shot noise originates from the granularity of the electron charge. Each electron can transmit or reflect from the scattering region, giving rise to partition noise. Analogous to hailstones falling on a tin roof, the electronic current will experience fluctuations. Writing the electrical current as $I = GV + \delta I(t)$, the current fluctuates on a very fast timescale, $\tau_0 = h/eV$, that is much shorter than any other timescale in the problem. Consequently, we can treat the fluctuations as uncorrelated on the timescale of the detection process, also called the "white noise" approximation. The strength of the shot noise is characterized by

$$S_I = \int dt \langle \delta I(t+\tau)\delta I(\tau)\rangle, \tag{5.7}$$

where S_I is independent of τ by stationarity of the process. The quantity S_I may be interpreted as the zero frequency noise power. The fermionic nature of the particles gives rise to an exclusion process, so the noise power is given by (Blanter and Büttiker, 2000).

$$S_I = (eV)\frac{4e^2}{h}\mathcal{T}(1-\mathcal{T}). \tag{5.8}$$

In the limit where $k_B\Theta \ll eV \ll E_F$, we consider for simplicity. We note that if either $\mathcal{T}$ is 0 or 1, there is no noise because all electrons are either reflected or transmitted; otherwise, the partitioning of the electron current is noisy. Note that $S_I = 2e\langle I\rangle(1-\mathcal{T})$, where $\langle I\rangle$ is the average electrical current. The expression $e\langle I\rangle$ is the Schottky expression for the electronic noise of vacuum tubes, resulting from Poissonian statistics of well-spaced electrons. The multiplicative factor of $1-\mathcal{T}$ for mesoscopic circuits indicates that the statistics are sub-Poissonian for this detector, as is generically the case for coherent electronic conductors.

Returning to the problem of quantum detection, we seek to distinguish currents I_L from I_R. Let us introduce the measured quantity,

$$\mathcal{Q} = \int_0^T dt' I(t'), \tag{5.9}$$

https://doi.org/10.1017/9781009103909.006 Published online by Cambridge University Press

which may be interpreted as the accumulated charge from a measurement lasting a time T. Supposing no tunneling occurs for the DQD ($\Delta = 0$) in the simplest case. Then the signal accumulated is $\mathcal{Q}_L - \mathcal{Q}_R = T(I_L - I_R)$, while the variance of $\mathcal{Q}$ is given by

$$\langle \delta \mathcal{Q}^2 \rangle = \int_0^T dt_1 dt_2 \langle \delta I(t_1) \delta I(t_2) \rangle. \tag{5.10}$$

Using the stationary nature of the process and changing variables to $t_s = (t_1 + t_2)/2, t_d = t_1 - t_2$, we have in the limit where T is long compared to τ_0 the result $\langle \delta \mathcal{Q}^2 \rangle \approx TS_I$. Regardless of the statistics of $\delta I(t)$ (under certain assumptions about how quickly the tails of the distribution fall off), the central limit theorem dictates that the distribution of $\mathcal{Q}/T$ limits to a Gaussian with the mean of I_L or I_R (depending on the initial state of the DQD), and a variance as shown earlier.

We now appeal to the concept of the signal-to-noise ratio, introduced in the previous chapter in Section 4.4. The detector's signal-to-noise ratio, distinguishing the electron being on the left or right dot, is given by

$$\mathcal{R} = \frac{\mathcal{Q}_L - \mathcal{Q}_R}{\sqrt{\langle \delta Q^2 \rangle}}. \tag{5.11}$$

In principle, one can have different noise powers for the two different configurations. However, in the weakly responding detector limit, there is little difference between the two noise powers, so we can use the formula (5.8) for the noise power, where the transmission is taken to be the average, $\mathcal{T} = (\mathcal{T}_L + \mathcal{T}_R)/2$. Thus, we find a simplified expression for the SNR,

$$\mathcal{R} = \sqrt{\frac{T}{\tau_0}} \frac{\mathcal{T}_L - \mathcal{T}_R}{\sqrt{\mathcal{T}(1 - \mathcal{T})}}, \tag{5.12}$$

which grows as the square root of the time of the duration of the experiment, divided by the fast correlation time of the transport, and also depends on the dimensionless ratio of combinations of the transmission coefficient.

The preceding SNR gives a new timescale to the problem: a characteristic time needed to distinguish the signal from the background shot noise. It is defined by letting $\mathcal{R} = k$, where k is a constant of order 1. Shortly, we will use $k = 2$. Solving (5.12) for the associated time gives

$$\tau_m = \frac{k^2 S_I}{(I_L - I_R)^2}. \tag{5.13}$$

We call this timescale the *characteristic measurement time*, not to be confused with the duration of the measurement. We notice that, if $I_L \to I_R$, the characteristic measurement time diverges, so it takes longer and longer to distinguish

https://doi.org/10.1017/9781009103909.006 Published online by Cambridge University Press

the small signal from the noise. The characteristic measurement time is an important timescale in describing the quantum state dynamics of the DQD during the measurement process.

Recalling the form of the transmission of the QPC for a saddle-point contact potential (5.5), notice that the noise power S_I depends on the combination

$$\mathcal{T}(1-\mathcal{T}) = \frac{e^{-\epsilon}}{(1+e^{-\epsilon})^2}. \tag{5.14}$$

This function has its maximum at the point $\epsilon = 0$, corresponding to $\mathcal{T} = 1/2$, which is also the point of highest sensitivity! In order to find at what point the SNR is highest, we consider the linear response limit, so we can approximate

$$I_L - I_R = \frac{\partial I}{\partial \epsilon}\delta\epsilon, \tag{5.15}$$

where $\delta\epsilon$ accounts for the small shift in the potential energy V_0 for the two positions the DQD electron induces, $\delta\epsilon = -2\pi\delta V_0/\hbar\omega_x$. Once the device structure is made, the geometric capacitances and potential landscape of the sample are fixed, but the transmission of the contact can be controlled with a top gate, shifting the overall value of V_0 with an applied gate voltage. Recalling the result (5.6), the measurement time is given by

$$\tau_m = \frac{4k^2\tau_0}{\delta\epsilon^2}\cosh^2(\epsilon/2). \tag{5.16}$$

The assumption that $\delta\epsilon \ll 1$ guarantees that $\tau_m \gg \tau_0$. For $\delta\epsilon$ fixed by the geometry of the sample, this quantity is minimized at $\epsilon = 0$, corresponding to $\mathcal{T} = 1/2$. Consequently, the fastest measurement one can make with this detector is for a half-open channel, despite the fact the noise is largest there. This fact comes from the sensitivity of the detector rapidly degrading as one approaches either the open or closed contact limit.

5.2 Measuring the State of a Superconducting Quantum Circuit with Electromagnetic Radiation

Another physical system that emerged in the early 2000s that is both a flexible laboratory for quantum measurement science and a promising candidate for quantum computing architectures is the circuit quantum electrodynamics architecture (cQED), as realized by superconducting circuits (Blais et al., 2004). While bearing many similarities to QED systems constructed from ultra-cold atoms, the electrical circuit version has a life of its own, allowing access to many parameter regimes difficult to implement in atomic systems and thus enabling new types of experiments. The basic architecture consists of a superconducting circuit embedded in a

https://doi.org/10.1017/9781009103909.006 Published online by Cambridge University Press

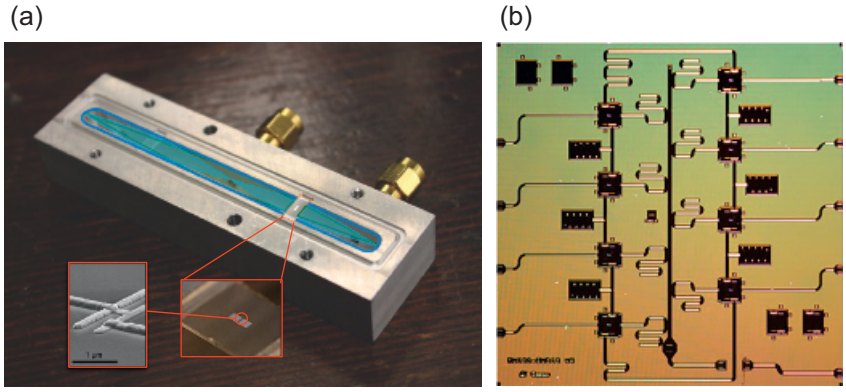

Figure 5.3 (a) A typical transmon qubit in a 3D geometry. A submicron Josephson tunnel junction is connected with two large paddles, which form the shunting capacitor and also an antenna to control the coupling to the electromagnetic field in the cavity. Shown here is half of a rectangular aluminum cavity, which is sandwiched together with the chip placed on a ledge in the center. (b) The transmon qubit can also be interfaced with a 2D cavity formed by a transmission line resonator on a planar chip. Shown here are eight transmon qubits on a 1-cm-square silicon chip connected via individual coupling capacitors to a single resonator bus.

microwave frequency cavity, either a 3D realization or a planar resonator colocated with the circuit on a semiconductor substrate.

As a canonical example, we consider a superconducting transmon qubit in a microwave resonator. In the previous chapter, we treated the case of a phase qubit, which, as its name implies, is well described by the dynamics of a fictitious particle in a tilted sinusoidal potential with a coordinate given by the Josephson junction phase. Qubits can also be constructed where the charge n on an isolated superconducting grain is a well-defined quantum number rather than the phase φ. The charge basis effectively reflects the eigenstates of a quantum circuit when the charging energy E_C, the energy associated with transferring a charge on/off the grain, is much larger than the Josephson energy E_J, which represents the energy associated with a Cooper pair tunneling across the junction. Conversely, states of definite phase are appropriate in the opposite limit. The ground state of a Cooper box (Vion, 2004) with $E_J \sim E_C$ was first probed in 1996, a superposition of ground and excited states was demonstrated in 1999, an improved version already fitted with single-shot readout and protection against dephasing was demonstrated in 2002, and the now ubiquitous transmon version with $E_J/E_C \sim 10 - 100$ appeared in 2006. For a description of the transmon, let us start with an isolated Josephson junction shunted by a capacitor C_S and charged biased via a gate capacitor C_g. The junction itself has a self-capacitance C_J and inductive energy E_J. The shunt capacitance allows control of the qubit frequency with the added benefit of shifting a

https://doi.org/10.1017/9781009103909.006 Published online by Cambridge University Press

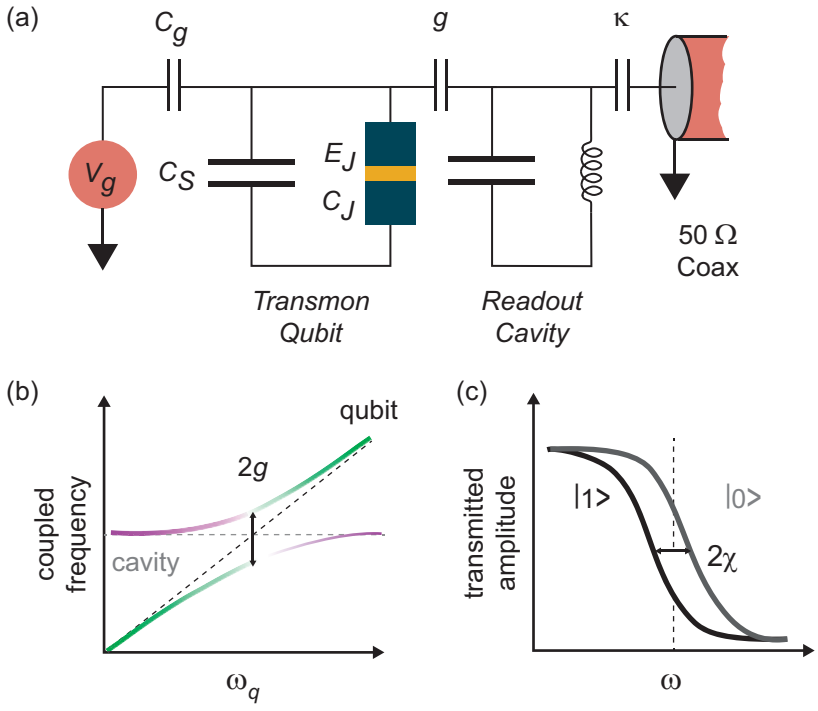

Figure 5.4 (a) Equivalent circuit of a transmon qubit formed by a Josephson junction shunted by a capacitor C_S and connected to a readout cavity. Qubit transitions are driven by an external voltage V_g, coupled via a capacitor C_g. The qubit-cavity coupling is parameterized by g, and the cavity decay rate to an external feedline is given by κ. (b) The frequencies of the coupled qubit-cavity system are plotted as a function of the qubit frequency for fixed cavity frequency. On resonance, an avoided crossing with splitting $2g$ is present. (c) In the dispersive limit, the qubit state pulls the bare cavity frequency, resulting in a quantum-state-dependent phase shift when the cavity is probed in transmission.

large fraction of the stored electromagnetic energy into a lower-loss capacitance, say one with a vacuum dielectric rather than an amorphous film. The Hamiltonian of the circuit can be written as

$$H = 4E_C(n - n_g)^2 - E_J \cos(\varphi), \tag{5.17}$$

where n is the Cooper pair charge on the circuit, $n_g = C_g V_g/2e$ is the charge bias expressed in Cooper pairs applied by an external voltage source V_g, and $E_C = e^2/2(C_S+C_J)$ is the charging energy which has contributions from both the junction capacitance and the external shunt.

This Hamiltonian can solved analytically in the phase basis using Mathieu functions (Koch et al., 2007). When $E_J/E_C < 1$, the circuit realizes a charge qubit and

https://doi.org/10.1017/9781009103909.006 Published online by Cambridge University Press

the energy difference between the ground and first excited states is highly sensitive to charge. The transmon operates with $E_J/E_C \sim 100$, where the lowest two levels are relatively insensitive to charge noise in the circuit environment, resulting in a dramatic improvement of coherence times from ns to hundreds of μs. The price to pay, so to speak, for this noise resilience is a reduction in anharmonicity. Fortunately, the charge dispersion is exponentially suppressed in E_J/E_C while the anharmonicity is proportional to $(E_J/E_C)^{-1/2}$. For a qubit with a frequency in the few GHz range, the frequency difference between adjacent pairs of qubit levels is ~ 100 MHz.

In the transmon limit, we can ignore the dependence of the Hamiltonian on offset charge, and truncate to leading nonlinear order in the potential (Blais et al., 2021) to obtain this approximate form:

$$\hat{H} = 4E_C n^2 + \frac{1}{2}E_J\varphi^2 - \frac{1}{24}E_J\varphi^4. \tag{5.18}$$

The first two terms essentially describe a harmonic oscillator with a nonlinear correction given by the third term. We can thus introduce creation and annihilation operators, $\hat{b}^\dagger$ and $\hat{b}$, to quantize the charge and phase operators using

$$\hat{\varphi} = \left(\frac{2E_C}{E_J}\right)^{1/4}(\hat{b}^\dagger + \hat{b}), \quad \hat{n} = \frac{i}{2}\left(\frac{E_J}{2E_C}\right)^{1/4}(\hat{b}^\dagger - \hat{b}). \tag{5.19}$$

The creation and annihilation operators obey the commutation relation $[\hat{b}, \hat{b}^\dagger] = 1$, so the number and phase operators obey the canonical commutation relation $[\hat{\varphi}, \hat{n}] = i$. Substituting these expressions into (5.18) and discarding any terms that do not conserve excitation number and would be oscillating in a rotating frame of reference, we obtain

$$\hat{H} = \hbar\omega_q \hat{b}^\dagger\hat{b} - \frac{E_C}{2}\hat{b}^\dagger\hat{b}^\dagger\hat{b}\hat{b}. \tag{5.20}$$

Here the qubit frequency associated with the lowest two levels

$$\hbar\omega_q = \sqrt{8E_J E_C} - E_C$$

is effectively the frequency of plasma oscillations in the Josephson potential offset by a Lamb shift of E_C. Notably, transitions to higher states are shifted by the second term that represents a Kerr-type nonlinearity.

To read out the state of the qubit, we couple it to a cavity. For simplicity, we can approximate the system as being described by the Jaynes–Cummings model for a spin 1/2 particle, thus only considering the two lowest states of the transmon coupled to a single mode of a bosonic field. In this limit, we can write the state of the qubit by a Pauli operator, say $\hat{\sigma}_z$. The simplified Hamiltonian for the coupled system is given by

https://doi.org/10.1017/9781009103909.006 Published online by Cambridge University Press

$$\hat{H} = \hbar\omega_c \hat{a}^\dagger \hat{a} + \hbar\omega_q \frac{\hat{\sigma}_z}{2} + \hbar g(\hat{a}^\dagger + \hat{a})(\hat{\sigma}_+ + \hat{\sigma}_-). \tag{5.21}$$

Here, the creation and annihilation operators $\hat{a}^\dagger$ and $\hat{a}$ refer to the excitations of the electromagnetic field, and $\hat{\sigma}_+$ and $\hat{\sigma}_-$ excite and relax the state of the two-level qubit described by $\hat{\sigma}_z$. The last term parameterizes the interaction between the qubit and the cavity and is of the form $\hat{\mathbf{p}} \cdot \hat{\mathbf{E}}$, which describes the typical interaction of a dipole with quantum operator $\hat{p} = \hat{\sigma}_+ + \hat{\sigma}_-$ with an electric field $\hat{E} = E_0(\hat{a}^\dagger + \hat{a})$ with zero-point-fluctuation amplitude E_0. Here we align the field in one direction and drop the vector nature of the field and dipole moment. The energy scales in the problem are set by the cavity frequency ω_c, the qubit frequency ω_q, and the light–matter coupling strength g. To further simplify (5.21), we can expand the product in the last term and drop products that do not conserve excitation number. These would correspond to transitions with energies much larger than the coupling strength. The Hamiltonian written in this interaction picture with respect to the first two terms of the Hamiltonian, or rotating frame, where we have dropped counterrotating terms is

$$\hat{H} = \hbar\omega_c \hat{a}^\dagger \hat{a} + \hbar\omega_q \frac{\hat{\sigma}_z}{2} + \hbar g(\hat{a}^\dagger \hat{\sigma}_- + \hat{a}\hat{\sigma}_+). \tag{5.22}$$

There are two basic decay processes in this system, parameterized by Γ, the spontaneous emission rate of the qubit, and κ, the cavity decay rate due to coupling to the external environment. We can express the coupling constant g in terms of circuit parameters,

$$g = \omega_c \frac{C_g}{C_J + C_S} \left(\frac{E_J}{2E_C}\right)^{1/4} \sqrt{\frac{\pi Z_c}{R_Q}}, \tag{5.23}$$

where Z_c is the impedance of the cavity mode and $R_Q = h/e^2$ is the resistance quantum.

As mentioned earlier, we can view the coupling energy $\hbar g$ as arising from a dipole interaction between the transmon and the vacuum electric field. To pen a dipole moment p_0, we can assume a characteristic length l associated with the motion of a Cooper pair in the qubit, yielding

$$p_0 = 2el \left(\frac{E_J}{32E_C}\right)^{1/4}, \quad E_0 = \frac{\omega_c}{l} \frac{C_g}{C_J + C_S} \sqrt{\frac{\hbar Z_c}{2}}. \tag{5.24}$$

Both of these quantities can be made large by appropriate circuit design. The distance a charge travels in a superconducting circuit is on a mesoscopic rather than an atomic length scale, giving rise to a large dipole moment which is efficiently coupled to volume occupied by the vacuum electric field, E_0. Thus, in electrical circuits, the coupling g can be made larger than both of these decay rates to

https://doi.org/10.1017/9781009103909.006 Published online by Cambridge University Press

achieve "strong coupling," where $g > \Gamma, \kappa$ (Wallraff et al., 2004). This regime is considerably more difficult to achieve in naturally occurring atomic systems which have a much smaller electric dipole moment, with the atom only occupying a small volume of the electric field. We note that while the two-level approximation captures many of the basic features of a cQED system, many important effects trace their origin to the additional quantized levels typically present in a superconducting circuit. Furthermore, cQED systems can also reach "ultrastrong" coupling where the hybridized states of the system involve multiple cavity levels. In addition to enabling more sophisticated tests of light–matter interaction, the presence of additional levels can also add functionality for both encoding and measuring quantum information.

We consider two basic limits of the Jaynes–Cummings model as referenced by the detuning $\Delta = \omega_q - \omega_c$. When $\Delta = 0$, the qubit and cavity are maximally entangled and the collective excitations are polariton-like. One cannot distinguish the individual character of either the cavity or the qubit. This regime has been used to study the radiative relaxation of an atom in squeezed vacuum. Gardiner calculated the variation of the spontaneous emission decay rate of an atom when coupled to an environment with intrinsic structure (Gardiner, 1986). For the case of quadrature squeezing, as demonstrated by Murch and coworkers, the transverse decay rate of a superconducting qubit varies depending on whether it is coupled to the quadrature with enhanced or suppressed fluctuations (Murch et al., 2013a). This experiment is very difficult to conduct using atomic systems interacting with free-space radiation as the vacuum in many spatial modes has to be squeezed and efficiency coupled. In the case of a superconducting qubit strongly interacting on resonance with a cavity, the system is essentially an artificial atom with a large electric dipole moment in a one-dimensional waveguide and can be readily coupled with a superconducting parametric amplifier generating a squeezed-state output. In this case, no signal is fed to the amplifier and it is only used to squeeze vacuum at its input. Superconducting parametric amplifiers are discussed later in Chapter 8 of this text.

More commonly, cQED systems operate in the dispersive limit with finite detuning Δ. When the detuning is large compared to the coupling strength g, the Jaynes–Cummings model can be approximated as

$$\hat{H} \approx \frac{1}{2}\hbar\left(\omega_q + \frac{g^2}{\Delta}\right)\hat{\sigma}_z + \hbar\omega_c(\hat{a}^\dagger\hat{a} + \frac{1}{2}) + \hbar\frac{g^2}{\Delta}\hat{\sigma}_z\hat{a}^\dagger\hat{a}, \tag{5.25}$$

as you will show in Exercise 5.6.4. The mutual interaction between the electromagnetic field and the qubit results in a modification of the frequencies of both systems. The terms in the Hamiltonian can be regrouped in different ways to make this apparent. From the point of view of the cavity, we can write

https://doi.org/10.1017/9781009103909.006 Published online by Cambridge University Press

$$\hat{H} \approx \frac{1}{2}\hbar\left(\omega_q + \frac{2g^2}{\Delta}\hat{a}^\dagger\hat{a} + \frac{g^2}{\Delta}\right)\hat{\sigma}_z + \hbar\omega_c\left(\hat{a}^\dagger\hat{a} + \frac{1}{2}\right), \tag{5.26}$$

where the qubit frequency has been shifted by g^2/Δ – this is a Lamb shift (Lamb and Retherford, 1947), caused by the interaction of the qubit with the vacuum fluctuations of the cavity. The presence of photons in the cavity further shifts the qubit frequency via the ac Stark effect (Autler and Townes, 1955). We can also view the interaction from the viewpoint of the qubit,

$$\hat{H} \approx \frac{1}{2}\hbar\omega_q\hat{\sigma}_z + \hbar\left(\omega_c + \frac{g^2}{\Delta}\hat{\sigma}_z\right)\left(\hat{a}^\dagger\hat{a} + \frac{1}{2}\right). \tag{5.27}$$

Here the resonant frequency is pulled by a dispersive shift $\pm\chi$ whose magnitude per photon is given by g^2/Δ. The sign of the effect depends on the state of the qubit, as reflected by the value of $\hat{\sigma}_z$.

This frequency shift forms the basis for a convenient measurement of the qubit state when the cavity is irradiated by a microwave tone. The magnitude of this shift also depends on average number of photons $\bar{n} = \langle\hat{a}^\dagger\hat{a}\rangle$ in the cavity. When an incident microwave signal is scattered off the qubit-cavity system, the outgoing wave is shifted in phase in a qubit-state-dependent fashion. For a small displacement in cavity frequency, we can estimate the expected angular response when the cavity is probed in a transmission measurement. We can express the phase response θ of the cavity as a function of the probe frequency ω and the decay rate to an external waveguide κ using

$$\theta = \arctan\left(\frac{2}{\kappa}(\omega_0 - \omega)\right), \tag{5.28}$$

where the bare cavity resonant frequency is ω_0. If the cavity is probed at ω_0, which is now the average of the dressed cavity frequencies with the qubit in its ground and excited states, we should ideally observe a total phase shift $4\chi/\kappa$.

Much like in the Stern–Gerlach experiment, repeating the measurement results in a histogram of values for microwave signal phase. The width of these histograms are a result of the measurement apparatus, which has fluctuations. In an idealized measurement, there would be no technical noise due to imperfections of the detector and only unavoidable quantum fluctuations would be present. If the histograms corresponding to the two qubit states are separated by greater than their width, a projective measurement is realized. Conversely, overlapping histograms realize a partial or weak measurement of the system.

A number of experimental parameters can be varied to smoothly go from one regime to the other. For a given coupling g, a larger frequency detuning Δ reduces the qubit-induced dispersive shift. Reducing the number of photons in the cavity also reduces the displacement of the histograms. Finally, the measurement time

https://doi.org/10.1017/9781009103909.006 Published online by Cambridge University Press

can be varied to narrow the histogram width, provided the measurement is not dominated by technical noise. The power signal-to-noise ratio $\mathcal{R}^2$ is a good proxy for the measurement strength and is obtained by taking the square of the ratio of the histogram separation to histogram standard deviation, as measured in amplitude units of the detected microwave field, and can be compactly expressed as

$$\mathcal{R}^2 = 64\chi^2 \left(\frac{\bar{n}T}{\kappa}\right). \tag{5.29}$$

Here, T is the measurement duration, and this expression assumes perfect measurement efficiency. Indeed, the use of near-quantum-noise-limited superconducting amplifiers has proven critical for implementing weak measurements where information is not lost into unmonitored degrees of freedom. In contrast, for situations with extra added noise or lost information, the measurement histograms overlap, but this is not a faithful weak measurement of the system, but rather the hallmark of an inefficient setup. To paraphrase Schrödinger, there is a difference between a shaky or out-of-focus photograph and a snapshot of clouds and fog banks (Trimmer, 1980).

5.3 Stochastic Schrödinger and Master Equations

Now that the physical systems have been outlined and discussed in detail, we will discuss the quantum state dynamics arising from these detection processes. Despite their clear differences, we will be able to describe both the QPC/DQD system and the cQED system with microwave readout in a unified way. We can consider both detection processes of the quantum systems as a kind of scattering process, where the scattering matrix elements depend on the qubit state. In the QPC/DD process, we will detect a change in the transmission coefficient, while in the cQED case, we will detect a phase shift of the optical readout.

Quantum State Change for the QPC/DQD Case in the Single Electron Limit

In the QPC/DQD case, the elementary process is an individual electron incident from the source electrode in a state with energy near the Fermi energy, described by state $|\text{in}\rangle$, with the qubit in state $|\psi\rangle = \alpha|L\rangle + \beta|R\rangle$. The scattering process maps this input state into an output scattering state,

$$|\text{in}\rangle(\alpha|L\rangle + \beta|R\rangle) \rightarrow \alpha(r_L|S\rangle + t_L|D\rangle)|L\rangle + \beta(r_R|S\rangle + t_R|D\rangle)|R\rangle, \tag{5.30}$$

where states $|S\rangle, |D\rangle$ are asymptotic scattering states corresponding to electrons ending in the source (S, reflected) or drain (D, transmitted) of the conductor. Here

https://doi.org/10.1017/9781009103909.006 Published online by Cambridge University Press

also, t_j, r_j where $j = L, R$ are the transmission or reflection amplitudes that depend on the qubit state and can be seen as elements of a scattering matrix $\overline{\overline{\mathbf{S}}}_j$,

$$\begin{pmatrix} b_S \\ b_D \end{pmatrix} = \overline{\overline{\mathbf{S}}}_j \begin{pmatrix} a_S \\ a_D \end{pmatrix}, \qquad \overline{\overline{\mathbf{S}}}_j = \begin{pmatrix} r_j & \bar{t}_j \\ t_j & \bar{r}_j \end{pmatrix}. \tag{5.31}$$

The scattering matrix maps the incoming scattering state **a** to the outgoing scattering states **b**. While the elements t_j, r_j correspond to transmission and reflection amplitudes for an electron incident from the source, the elements $\bar{t}_j, \bar{r}_j$ correspond to transmission and reflection amplitudes for an electron incident from the drain. The scattering matrix is unitary, which relates some of the matrix elements to each other.

The resulting state from the scattering process (5.30) results in entanglement between the position of the scattering electron and the left/right orientation of the electron in the DQD. The electron's transport state is detected as contributing to the electrical current in the conductor, which can be viewed as making a projection of the electron onto the source (S) or drain (D). It follows from our discussion in Chapter 3 that the measurement operators, expressed in the $|L\rangle, |R\rangle$ basis, are given by the matrices

$$\overline{\overline{\Omega}}_S = \begin{pmatrix} r_L & 0 \\ 0 & r_R \end{pmatrix}, \qquad \overline{\overline{\Omega}}_D = \begin{pmatrix} t_L & 0 \\ 0 & t_R \end{pmatrix}. \tag{5.32}$$

Consequently, we can write the E_j matrices as follows:

$$\overline{\overline{\mathbf{E}}}_S = \overline{\overline{\Omega}}_S^{\dagger} \overline{\overline{\Omega}}_S = \begin{pmatrix} R_L & 0 \\ 0 & R_R \end{pmatrix}, \qquad \overline{\overline{\mathbf{E}}}_D = \overline{\overline{\Omega}}_D^{\dagger} \overline{\overline{\Omega}}_D = \begin{pmatrix} T_L & 0 \\ 0 & T_R \end{pmatrix}, \tag{5.33}$$

where $T_j = |t_j|^2, R_j = |r_j|^2$. We notice that the coarse-grained position of the electron serves as an effective qubit meter in the preceding analysis, similar to Exercise 3.7.2. Next, the new quantum state, given the electron is found in the drain, is

$$|\psi_D'\rangle = \frac{\hat{\Omega}_D|\psi\rangle}{||\hat{\Omega}_D|\psi\rangle||} = \frac{t_L\alpha|L\rangle + t_R\beta|R\rangle}{\sqrt{T_L|\alpha|^2 + T_R|\beta|^2}}, \tag{5.34}$$

while the new quantum state, given the electron is found in the source, is

$$|\psi_S'\rangle = \frac{\hat{\Omega}_S|\psi\rangle}{||\hat{\Omega}_S|\psi\rangle||} = \frac{r_L\alpha|L\rangle + r_R\beta|R\rangle}{\sqrt{R_L|\alpha|^2 + R_R|\beta|^2}}. \tag{5.35}$$

To complete the analysis, the probability P of finding the electron in the drain D (or source S) is given by

$$P(D) = T_L|\alpha|^2 + T_R|\beta|^2, \qquad P(S) = R_L|\alpha|^2 + R_R|\beta|^2. \tag{5.36}$$

https://doi.org/10.1017/9781009103909.006 Published online by Cambridge University Press

As before, we can view this as an expression of the law of total probability. It turns out from symmetry considerations that, if the QPC is spatially symmetric, the scattering matrix elements are real, which gives the optimal efficiency, as we will see later on.

Quantum State Change for the cQED Dispersive Limit Case

A similar analysis can be done for the cQED setup in the dispersive limit. We consider a coherent state of light at microwave frequencies that is sent from a microwave source to the cavity via a transmission line. If the frequency of the light is near the resonant frequency of the cavity, it will enter it for a time, interact with the qubit, and then leave the cavity. The altered light can then be amplified and examined. In the dispersive limit, no energy is exchanged between qubit and cavity, but the interaction can give a conditional phase shift to the coherent state. We begin the analysis with the qubit in state $|\psi\rangle = a|0\rangle + b|1\rangle$, and the cavity coherent state (taken as the meter) in state $|\alpha\rangle$, where $|\alpha|^2$ characterizes the average number of photons in the state. The resulting interaction takes the form

$$(a|0\rangle + b|1\rangle)|\alpha\rangle \rightarrow a|0\rangle|\alpha_0\rangle + b|1\rangle|\alpha_1\rangle, \tag{5.37}$$

where the modified coherent states are given by

$$|\alpha_j\rangle = |\alpha e^{i\theta_j}\rangle. \tag{5.38}$$

Here, θ_j are the phase shifts acquired by the interaction, which are related to the product of the dispersive shift χ and the interaction time of the system and meter. The states of the cavity and the qubit are now entangled, and we assume the cavity is sufficiently lossy that the light field quickly leaks out without further interaction with the qubit. This will be satisfied if $\kappa \gg \chi$. The light state is now measured by an amplification process, which will be described in detail in Chapters 7 and 8. For now, we will describe the result of the process as a projection of the coherent state onto one of its quadrature variables. Defining a position-like operator (in the context of the quantum harmonic oscillator) $\hat{X} = (\hat{a}+\hat{a}^\dagger)/\sqrt{2}$ for the light field, we will project on $\hat{\Pi}_x = |x\rangle\langle x|$, where $|x\rangle$ are the eigenstates of operator $\hat{X}$ with eigenvalues x, a continuous variable. The amplifier has the freedom to amplify along any quadrature that is a linear combination of $\hat{a}$ and $\hat{a}^\dagger$, but that is also equivalent to changing the phase of the input coherent state, so we choose to keep the amplifier quadrature fixed and vary the input phase. It is important to note that the phase is relative to an external clock which is an important part of the amplification process. Taking the phase shift from the qubit to be $\theta_j = \pm\theta_0$ (typically a very small angle), the choice of phase for α can result in varying information revealed about the qubit state, ranging from 0 (when α is real) to a maximal value (when α is imaginary).

https://doi.org/10.1017/9781009103909.006 Published online by Cambridge University Press

We note the total phase shift is $2\theta_0$. This is because the projection onto the real axis results in partially distinguishable distributions, depending on the phase of α. Thus, we can view the meter as a continuous degree of freedom, like the position of the Stern–Gerlach device, or the optical beam position for the birefringence case. From the methods of Chapter 3, the measurement operator is therefore given by

$$\hat{\Omega}_x = \langle x|\alpha_0\rangle|0\rangle\langle 0| + \langle x|\alpha_1\rangle|1\rangle\langle 1|. \tag{5.39}$$

The coefficients $\langle x|\alpha_j\rangle$ are simply the wavefunctions of the two coherent states. These are given by

$$\langle x|\alpha_j\rangle = \frac{1}{\pi^{1/4}} \exp\left[-\frac{1}{2}\left(x - \sqrt{2}\mathrm{Re}(\alpha_j)\right)^2 + i\,\mathrm{Im}(\alpha_j)\left(\sqrt{2}x - \mathrm{Re}(\alpha_j)\right)\right]. \tag{5.40}$$

From this wavefunction, it can be verified that $\langle x\rangle_j = \sqrt{2}\mathrm{Re}(\alpha_j)$, and $\mathrm{Var}[x] = 1/2$, corresponding to the quantum vacuum fluctuations of the coherent state of light. This corresponds to the $\overline{\overline{E}}_x$ operator given in matrix form by

$$\overline{\overline{E}}_x = \begin{pmatrix} |\langle x|\alpha_0\rangle|^2 & 0 \\ 0 & |\langle x|\alpha_1\rangle|^2 \end{pmatrix}. \tag{5.41}$$

The measurement operator allows us to find the probability distribution P for x, when the qubit is in a coherent superposition,

$$P(x) = |a\langle x|\alpha_0\rangle|^2 + |b\langle x|\alpha_1\rangle|^2, \tag{5.42}$$

so we have $\langle x\rangle = \sqrt{2}[|a|^2\mathrm{Re}(\alpha_0) + |b|^2\mathrm{Re}(\alpha_1)]$, and $\mathrm{Var}[x] = 1/2$. Let us choose $\alpha = i|\alpha|$ to get the best signal, corresponding to

$$\mathrm{Re}(\alpha_j) = \pm|\alpha|\sin\theta_0 \approx \pm\sqrt{\bar{n}}\theta_0, \tag{5.43}$$

for small values of θ_0, where $\bar{n}$ is the average number of photons in the cavity. Appealing to the concept of signal-to-noise ratio introduced in Section 4.4, we can quantify our ability to discriminate the two qubit states by taking the difference of the average detected signals, divided by their standard deviation,

$$\mathcal{R} = \frac{|\langle x\rangle_1 - \langle x\rangle_0|}{\sqrt{\mathrm{Var}[x]}} = 4\sqrt{\bar{n}}\theta_0. \tag{5.44}$$

This number is typically much less than 1. Given result x has been recorded for the result of operator $\hat{X}$ on the meter, the new system state is given by

$$|\psi'\rangle_x = \frac{\hat{\Omega}_x|\psi\rangle}{||\hat{\Omega}_x|\psi\rangle||} = \frac{\langle x|\alpha_0\rangle|0\rangle + \langle x|\alpha_1\rangle|1\rangle}{\sqrt{|\langle x|\alpha_0\rangle|^2 + |\langle x|\alpha_1\rangle|^2}}. \tag{5.45}$$

https://doi.org/10.1017/9781009103909.006 Published online by Cambridge University Press

5.4 Continuous Measurement

In both examples of the QPC/QDQ and the cQED systems, the previous two sections are not a realistic description of the actual measurements made, but are useful idealizations. In practice, the timescale of the electron passing the barrier $\tau_0 \sim h/eV$, or the duration of light in the cavity $\sim \kappa^{-1}$, is very short. It is, in fact, the cumulative effect of many electrons interacting with the system and forming a quasi-continuous noisy current $I(t)$, or the resulting voltage signal from the optical amplifier, forming a quasi-continuous noisy quadrature signal $x(t)$. We can pass from a discrete to quasi-continuous limit by time-indexing the result s_i, where we give a unified treatment by letting s be either I or x. In both cases, let us consider the time average over a duration T,

$$\bar{s}(T) = \frac{1}{N}\sum_{i=1}^{N} s_i = \frac{1}{T}\int_0^T dt\, s(t), \tag{5.46}$$

where we go over to a continuous description, $s(t_i) = s(t)$. From the central limit theorem, the distribution of the random variable $\bar{I}$ converges to a Gaussian (so long as the tails of the distribution of s_i do not decay too slowly), so we can specify the statistics with the mean and variance of $\bar{s}$, which depend only on the first and second moments of $s(t)$, depending on the qubit state

$$\langle s\rangle = \begin{cases} I_{L,R}, & \text{QPC/DQD,} \\ \sqrt{2}\mathrm{Re}(\alpha_{0,1}), & \text{cQED.} \end{cases} \tag{5.47}$$

Here the angle brackets are taken over a statistical ensemble. We take the time step discretization to be in units of the correlation time τ_0 for both systems, so the variables are uncorrelated in different time windows. The variance of $\bar{s}$ is given by

$$\mathrm{Var}[\bar{s}] = \sum_{i,j=1}^{N}\langle \delta s_i \delta s_j\rangle = \mathrm{Var[s]}/N = \frac{1}{(T)^2}\int_0^T \langle \delta s(t)\delta s(t')\rangle dt dt'. \tag{5.48}$$

The duration is $T = N\tau_0$, so we conclude that

$$\langle \delta s(t+\tau)\delta s(t)\rangle = S_s\delta(\tau), \tag{5.49}$$

in the white noise limit (assuming we consider times longer than the correlation time), where

$$S_s = \begin{cases} S_I, & \text{QPC/DQD,} \\ \tau_0/2, & \text{cQED.} \end{cases} \tag{5.50}$$

In the cQED case, we associate the correlation time with the timescale of the cavity ringing up or down, given by $\tau_0 = \kappa^{-1}$, while the phase shift due to the qubit is

https://doi.org/10.1017/9781009103909.006 Published online by Cambridge University Press

given by $\theta_0 = 2\chi/\kappa$ in the dispersive approximation. We then have the SNR for $T\bar{s}$ given by

$$\mathcal{R} = \begin{cases} \frac{(I_L - I_R)}{\sqrt{S_I}}\sqrt{T}, & \text{QPC/DQD}, \\ \frac{8\chi\sqrt{\bar{n}}}{\kappa}\sqrt{\kappa T}, & \text{cQED}. \end{cases} \tag{5.51}$$

A complementary, more detailed derivation of this result is given in Chapter 7. It is convenient to now shift and scale the $\bar{s}$ variable to make it symmetric and dimensionless. We define the continuous measurement result

$$r = \frac{2\bar{s} - (s_0 + s_1)}{s_0 - s_1}, \tag{5.52}$$

so when $s = s_0$, the result corresponds to $r = 1$, while when $s = s_1$, the result corresponds to $r = -1$. Given this convention, we define the characteristic measurement time τ_m such that the probability distributions $P_j(r)$ corresponding to $j = 0, 1$ are given by

$$P_j(r) = \sqrt{\frac{T}{2\pi\tau_m}} \exp\left[-\frac{T}{2\tau_m}(r \mp 1)^2\right]. \tag{5.53}$$

Here $j = 0, 1$ corresponds to $-, +$, respectively. The mean of r is ± 1, while its variance is τ_m/T. With this convention (corresponding to the choice $k = 2$ in (5.13)), the characteristic measurement times are given by

$$\tau_m = \begin{cases} \frac{4S_I}{(I_L - I_r)^2}, & \text{QPC/DQD}, \\ \frac{\kappa}{16\chi^2\bar{n}}, & \text{cQED}. \end{cases} \tag{5.54}$$

Quantum Trajectories: a First Look

Drawing on treatment of generalized quantum measurement, we can predict how the state will be disturbed with the measurement operator $\hat{\Omega}_r$, corresponding to finding a result r lying in a region of bin size Δr, so the probability is given by

$$P(r)\Delta r = \langle\psi|\hat{\Omega}_r^\dagger\hat{\Omega}_r|\psi\rangle = |\alpha|^2 P_0(r)\Delta r + |\beta|^2 P_1(r)\Delta r. \tag{5.55}$$

The new state is given by $|\psi'\rangle = \hat{\Omega}_r|\psi\rangle/||\hat{\Omega}_r|\psi\rangle||$. Notice that any factor appearing in $\hat{\Omega}_r$ that is common to both states may be dropped, because it will cancel out in the denominator during the renormalization. Consequently, we can simplify

$$\hat{\Omega}_r = \begin{pmatrix} \sqrt{P_0(r)\Delta r} & 0 \\ 0 & \sqrt{P_1(r)\Delta r} \end{pmatrix} \propto \hat{\Omega}'_r = \begin{pmatrix} e^{\frac{Tr}{2\tau_m}} & 0 \\ 0 & e^{-\frac{Tr}{2\tau_m}} \end{pmatrix}. \tag{5.56}$$

The form of $\hat{\Omega}'$ is illuminating: we see that if a result $r > 0$ is obtained, partial collapse toward state $|0\rangle$ occurs, while a result $r < 0$ gives partial collapse toward state $|1\rangle$.

https://doi.org/10.1017/9781009103909.006 Published online by Cambridge University Press

This behavior can be described with a differential equation. Let us define for simplicity the unnormalized state coefficients $\tilde{\alpha}, \tilde{\beta}$ (the true state can always be found by renormalizing). It then follows by taking a time derivative and letting $T \to 0$ that

$$\frac{d}{dt}\begin{pmatrix}\tilde{\alpha}\\ \tilde{\beta}\end{pmatrix} = \frac{r}{2\tau_m}\hat{\sigma}_z\begin{pmatrix}\tilde{\alpha}\\ \tilde{\beta}\end{pmatrix}. \tag{5.57}$$

The solution is easily found by integration,

$$\tilde{\alpha}(t) = \tilde{\alpha}(0)\exp\left(\frac{1}{2\tau_m}\int_0^t dt' r(t')\right), \quad \tilde{\beta}(t) = \tilde{\beta}(0)\exp\left(-\frac{1}{2\tau_m}\int_0^t dt' r(t')\right). \tag{5.58}$$

Consequently, only the time-integrated signal of $r(t)$ matters as time develops, that is, $\int^t dt' r(t')$. The integrated signal is also Gaussian with mean $t\langle\hat{\sigma}_z\rangle(0)$ and variance of $t\tau_m$. We will see later this property no longer holds once we add in a system Hamiltonian. Notice that we can make the prediction of the quantum state given that we are provided $r(t)$, for example by an experiment. However, we have seen that the probability distribution of r depends on the state, while the equation of motion for the state depends on the measurement result. We will learn how to deal with this full solution of the problem in the next section.

Describing Quantum Trajectories: Stochastic Differential Equations

The full solution of quantum trajectories described as a continuous stochastic process requires learning about the mathematical formalism behind stochastic processes, such as stochastic differential equations, Fokker–Planck equations, stochastic path integrals, and so on. Before launching into this, let us take a step back to the time-discretized case. We divide the timeline up into pieces of size Δt. The index $j = 1, \ldots, N$ stands for the time index, so the duration $T = N\Delta t$. The quantum trajectory is defined as an iterative map,

$$|\psi_{j+1}\rangle = \frac{\hat{\Omega}_{r_j}|\psi_j\rangle}{||\hat{\Omega}_{r_j}|\psi_j\rangle||}, \tag{5.59}$$

where the measurement result r_j is drawn from the probability (density)

$$P(r_j) = \langle\psi_j|\hat{\Omega}^\dagger_{r_j}\hat{\Omega}_{r_j}|\psi_j\rangle. \tag{5.60}$$

The set of results $\{r_j\}$, where $j = 1, \ldots, N$ is the measurement record, and the set of states $\{|\psi_j\rangle\}$ is the quantum trajectory. As $\Delta t \to 0$ this becomes a continuous process with a well-defined mathematical limit; but, of course, in experiments there is always a smallest timescale of the correlation time of the detector than which the considered time steps should always be longer. This is typical of all stochastic

https://doi.org/10.1017/9781009103909.006 Published online by Cambridge University Press

processes in nature. We can also add in unitary dynamics with a system Hamiltonian H_S via the unitary operator

$$\hat{\Omega}_{r_j} \to \hat{U}_j \hat{\Omega}_{r_j}, \qquad \hat{U}_j = e^{-i\Delta t H_s(t_j)/\hbar}, \tag{5.61}$$

where we assume $\Delta t H_s/\hbar$ is much smaller than the identity. The ordering of the operators does not matter at this stage, since the commutator of the two operators will be order Δt^2 and can be neglected.

Recalling Eqs. (5.53) and (5.49), we can introduce $r(t)$ as a time-dependent stochastic variable with mean $|\alpha|^2 - |\beta|^2$ that is uncorrelated with itself unless the time index is the same, with variance τ_m/T, where we consider a duration $T = \Delta t$ for the moment. Letting $\Delta t \to 0$ formally, we can write equivalently

$$r(t) = \langle \hat{\sigma}_z \rangle(t) + \sqrt{\tau_m}\xi(t). \tag{5.62}$$

Here, the variable $\xi(t)$ is a Gaussian random variable of zero mean and is delta-correlated in time,

$$\langle \xi(t) \rangle = 0, \qquad \langle \xi(t)\xi(t') \rangle = \delta(t - t'). \tag{5.63}$$

These definitions reproduce the statistics of $r(t)$. The singular nature of the noise as $\Delta t \to 0$ can lead to mathematical difficulties, so it is also convenient to introduce the Wiener increment ΔW, also a Gaussian random variable defined so that the variance is given by $\mathrm{Var}[\Delta W] = \mathrm{Var}[\Delta t\, r]/\tau_m = \Delta t$, which vanishes as the time interval limits to 0. We can then define

$$\xi(t) = \lim_{\Delta t \to 0} \frac{\Delta W}{\Delta t} = \frac{dW}{dt}. \tag{5.64}$$

We will return to the Wiener differential dW shortly.

We will now derive equations of motion for the normalized qubit state based on our first result (5.57). Let us generalize the treatment by going to a density matrix formulation of the problem and finding the stochastic equation of motion for the density matrix, with elements

$$\rho_{ij} = \frac{\langle i|\psi\rangle\langle\psi|j\rangle}{\langle\psi|\psi\rangle} = \frac{\psi_i \psi_j^*}{\sum_k |\psi_k|^2}, \tag{5.65}$$

expressed in the $|0\rangle, |1\rangle$ basis, where the normalization allows us to consider also the unnormalized state $|\psi\rangle$, and $\psi_i = \langle i|\psi\rangle$. We can now apply a time-derivative to ρ_{ij} and use the rules of calculus to find

$$\dot{\rho}_{ij} = \frac{\dot{\psi}_i \psi_j^* + \psi_i \dot{\psi}_j^*}{\sum_k |\psi_k|^2} - \frac{2\psi_i \psi_j^* (\sum_l (\dot{\psi}_l \psi_l^* + \psi_l \dot{\psi}_l^*)}{(\sum_k |\psi_k|^2)^2}. \tag{5.66}$$

https://doi.org/10.1017/9781009103909.006 Published online by Cambridge University Press

We assume at $t = 0$, the density matrix begins as the pure state

$$\hat{\rho} = \begin{pmatrix} |\alpha|^2 & \alpha\beta^* \\ \alpha^*\beta & |\beta|^2 \end{pmatrix}. \tag{5.67}$$

Inserting our previous results (5.57), we find the following differential equation for each matrix element,

$$\dot{\rho}_{00} = \frac{r}{\tau_m}\rho_{00} - \frac{r}{\tau_m}\rho_{00}(\rho_{00} - \rho_{11}), \tag{5.68}$$

$$\dot{\rho}_{11} = -\frac{r}{\tau_m}\rho_{11} - \frac{r}{\tau_m}\rho_{11}(\rho_{00} - \rho_{11}), \tag{5.69}$$

$$\dot{\rho}_{01} = (\dot{\rho}_{10})^* = -\frac{r}{\tau_m}\rho_{01}(\rho_{00} - \rho_{11}). \tag{5.70}$$

It is interesting to check that, since this is an equation for a normalized density matrix, the time derivative of the trace, given by $\dot{\rho}_{00} + \dot{\rho}_{11}$, is indeed exactly 0. It is often useful to reparameterize ρ for a qubit with the Bloch coordinates (x, y, z) defined by

$$\hat{\rho} = \frac{1}{2}\begin{pmatrix} 1+z & x-iy \\ x+iy & 1-z \end{pmatrix}, \tag{5.71}$$

or inverting the relation, $z = \rho_{00} - \rho_{11}, x = 2\mathrm{Re}(\rho_{01}), y = -2\mathrm{Im}(\rho_{01})$. All possible states (with trace 1, and eigenvalues between 0 and 1) must lay within a ball defined by $x^2 + y^2 + z^2 \leq 1$, with pure states residing on the surface, and mixed states inside the ball. We may reexpress the equations of motion for the qubit in these coordinates, as well as add in the effect of the system Hamiltonian $H_S = (\epsilon/2)\hat{\sigma}_z + (\Delta/2)\hat{\sigma}_x$, which may be accounted for as additional terms, corresponding to the Schrödinger equation, $d\hat{\rho}/dt = -i[H_S, \hat{\rho}]$, to give the unified equations

$$\dot{x} = -\frac{r}{\tau_m}xz - \epsilon y, \tag{5.72}$$

$$\dot{y} = -\frac{r}{\tau_m}yz + \epsilon x - \Delta z, \tag{5.73}$$

$$\dot{z} = \frac{r}{\tau_m}(1 - z^2) + \Delta y. \tag{5.74}$$

There equations are supplemented with the stochastic readout, given as a random variable, that depends on the qubit state as

$$r = \mathrm{Tr}[\hat{\rho}\hat{\sigma}_z] + \sqrt{\tau_m}\xi = z + \sqrt{\tau_m}\xi. \tag{5.75}$$

Thus, the readout traces the instantaneous value of qubit signal $z(t)$, but is masked by detector noise. Although the readout does not depend on x, y, knowledge of the initial state together with the system parameters allows us to predict the values of the entire state, given the noisy measurement readout $r(t)$. Inserting (5.75) into

https://doi.org/10.1017/9781009103909.006 Published online by Cambridge University Press

the preceding equations of motion then gives a complete description of the stochastic process of the continuously measured qubit as a set of coupled stochastic differential equations.

Solving the Stochastic Differential Equations

We must now enter a point of mathematical subtlety that has confused many a physicist. Namely, how can we construct solutions of equations of the form (5.72, 5.73, 5.74)? We must stress at the outset that the underlying physical prediction of the quantum state at a given time is perfectly well defined, as is clear from the discussion in Section 5.4. Nevertheless, when stochastic differential equations are written, they cannot be considered meaningful unless an "interpretation" is also given. The most common ones in the literature are the Itô and the Stratonovich interpretations. The interpretation refers to a problem that is encountered when trying to integrate these equations. We are faced with how to deal with expressions of the form $\int dt\xi(t)f(q(t))$, where q stands in for any system variable, and f is some function of the variable. Let us consider a generic stochastic differential equation of the form

$$\dot{q} = a(q) + b(q)\xi. \tag{5.76}$$

When $b(q)$ is nonconstant, this is sometimes referred to as multiplicative noise and causes the ambiguity mentioned before. Let us write a discretized version of this equation,

$$q_{k+1} - q_k = a(\bar{q}_k)\Delta t + b(\bar{q}_k)\Delta W_k, \tag{5.77}$$

where again, ΔW_k is the Wiener increment. Thus, the solution to $q(T)$ is given by the sum of increments,

$$\begin{aligned} q(T) &= (q_N - q_{N-1}) + (q_{N-1} - q_{N-2}) + (q_{N-2} - q_{N-3}) + \ldots + q_0 \\ &= q_0 + \sum_{k=0}^{N-1} a(\bar{q}_k)\Delta t + b(\bar{q}_k)\Delta W_k. \end{aligned} \tag{5.78}$$

The mathematical ambiguity comes into how to assign $\bar{q}_k$. We could assign it at the beginning of the interval (Itô convention, $\beta = 0$), or at the midpoint (Stratonovich convention, $\beta = 1/2$), or anywhere else we like,

$$\bar{q}_k = \beta q_{k+1} + (1 - \beta)q_k, \tag{5.79}$$

where $\beta \in [0, 1]$. Depending on how we choose this convention as $\Delta t \to 0$, the above increment sum will converge to different answers. This is due to the stochastic nature of ΔW_k, which is continuous, but not differentiable. Despite this seeming ambiguity, we must remember van Kampen's dictum, "From a physical point of

https://doi.org/10.1017/9781009103909.006 Published online by Cambridge University Press

view the Itô–Stratonovich controversy is moot" (Van Kampen, 1981). The point is that any stochastic differential equation that has nonlinear terms in it must also be supplemented by a convention about the choice of β. Without it, the stochastic differential equation is just a meaningless string of symbols.

It turns out that Eqs. (5.72, 5.73, 5.74) must be interpreted as Stratonovich-form stochastic differential equations, because we used the ordinary rules of calculus in the time derivative of ρ_{ij}. We can also shift the time increments by half a step and define the time derivative in a symmetrized form, $\dot{q} = [q(t+\delta t/2) - q(t-\delta t/2)]/\delta t$ in the Stratonovich interpretation. In order to use other choices of β, new forms of stochastic calculus must be applied. The most common one is Itô, which is typically favored by mathematicians, the subject of the next section, while physicists typically favor the Stratonovich interpretation because of its deeper, more physical origin. We will go into more detail about this point later in the chapter. Indeed, coming back again to van Kampen, "The final conclusion is that a physicist cannot go wrong by regarding the Itô interpretation as one of those vagaries of the mathematical mind that are of no concern to him." (Van Kampen, 1981). Nevertheless, because this interpretation is common in the quantum trajectory literature and in statistical physics more generally, we will discuss it now.

Introduction to Itô Stochastic Calculus

We begin by considering a continuous random walk, described by the variable $W(t)$, which is a random variable, with distribution

$$P(W) = \sqrt{\frac{2\pi}{t}} \exp\left(-\frac{W^2}{2t}\right). \tag{5.80}$$

This process can be developed by starting with $W = 0$ and adding the Wiener increment $\Delta W(t) = W(t_k + \Delta t) - W(t_k)$ repeatedly. The variance of Δt will simply add with each step, so the $t = N\Delta t$ variance of $W(t)$ is recovered. We can keep t fixed and take $N \to \infty$ while $\Delta t \to 0$. Each additional increment is statistically independent of all past values.

In the limit, Δt shrinks to the infinitesimal dt, and we define the limit of the Wiener increment to be $\Delta W \to dW$. Consequently, we can represent Eq. (5.77) as

$$dq = a(q)dt + b(q)dW \tag{5.81}$$

in this limit. Importantly, in the Itô interpretation, $\bar{q}$ is taken at q_k, while $\Delta W_k = W_{k+1} - W_k$, so we can say $b(q)$ is "nonanticipating." This convention then permits the nice simplification

$$\langle b(q)dW \rangle = 0, \tag{5.82}$$

https://doi.org/10.1017/9781009103909.006 Published online by Cambridge University Press

because the average over the noise involves integrating over W_{k+1}, which has zero mean, while $b(q_k)$ does not involve the next time step.

The variance of ΔW is Δt, indicating that we should regard ΔW to be of order $\sqrt{\Delta t}$ in expansions with respect to time. This is very important because the usual chain rule does not apply in Itô calculus. The correct procedure is to expand the relevant equations with respect to dt and dW, and to keep to first order in dt, but to second order with respect to dW. As $\Delta t \to 0$, we can drop terms $dt^2, dtdW$, and higher order. To see why this is, we return to the discrete time case, so time is labeled by t_k, and the duration Δt times the number of steps N is the total duration t. We define the stochastic integral

$$\int_0^t dW = \lim_{N\to\infty} \sum_{k=1}^{N} \Delta W_k = W(t), \tag{5.83}$$

where $W_k = W(t_k)$. Let us now consider the stochastic integral

$$X = \int_0^t dW^2 = \lim_{N\to\infty} \sum_{k=1}^{N} (\Delta W_k)^2. \tag{5.84}$$

The claim we made earlier is equivalent to $X = t$ exactly. Let us check this by first taking the statistical average of X,

$$\langle X \rangle = \lim_{N\to\infty} \sum_{k=1}^{N} \langle (\Delta W_k)^2 \rangle = \lim_{N\to\infty} N\Delta t = t. \tag{5.85}$$

If $X = t$ exactly, then the variance of X should be zero. Let us check that this is the case:

$$\mathrm{Var}[X] = \lim_{N\to\infty} \langle \sum_{k,l=1}^{N} (\Delta W_k)^2 (\Delta W_l)^2 \rangle - t^2. \tag{5.86}$$

We can simplify the first term as

$$\langle \sum_{k,l=1}^{N} (\Delta W_k)^2 (\Delta W_l)^2 \rangle = \sum_{k=1}^{N} \langle (\Delta W_k)^4 \rangle + \sum_{k\neq l=1}^{N} \langle (\Delta W_k)^2 \rangle \langle (\Delta W_l)^2 \rangle. \tag{5.87}$$

Here we use the fact that the Wiener increments at different times are uncorrelated, so their average product can be replaced by their product of averages. The average $\langle \Delta W_k^4 \rangle = 3\langle \Delta W^2 \rangle^2 = 3\Delta t^2$ is the fourth moment of a Gaussian distribution, while we can replace $\langle (\Delta W_k)^2 \rangle \langle (\Delta W_l)^2 \rangle = \Delta t^2$. We must now account for the fact that there are N of the fourth moment terms, while there are $N^2 - N$ of the $k \neq l$ terms, to find

$$\mathrm{Var}[X] = \lim_{N\to\infty} 3N\Delta t^2 + (N^2 - N)\Delta t^2 - t^2 = \lim_{N\to\infty} \frac{2t^2}{N} = 0. \tag{5.88}$$

https://doi.org/10.1017/9781009103909.006 Published online by Cambridge University Press

In the last equality, we have replaced $\Delta t = t/N$, keeping the time interval t fixed. This derivation justifies $dW^2 = dt$ as a deterministic replacement in the infinitesimal limit.

Stochastic Schrödinger Equation

We may now apply the above methods to derive the Itô form of the stochastic differential equations. In the infinitesimal limit, the measurement result $r(t)\Delta t$ is replaced by the increment dr, where

$$r(t)\Delta t \to dr = \langle \hat{\sigma}_z \rangle dt + \sqrt{\tau_m} dW. \tag{5.89}$$

The state update (5.56) can be expanded to second order in r:

$$\psi_j' = \psi \left(1 \pm \frac{dr}{2\tau_m} + \frac{1}{2} \frac{dr^2}{(2\tau_m)^2} \right) / |||\psi'\rangle||, \tag{5.90}$$

where $\psi_j = \tilde{\alpha}, \tilde{\beta}$, for $j = 0, 1$ respectively. Making the replacement $dW^2 = dt$ and dropping higher-order terms gives

$$\psi_j' = \psi_j \left(1 \pm \langle \hat{\sigma}_z \rangle \frac{dt}{2\tau_m} + \frac{dt}{8\tau_m} \pm \frac{dW}{2\sqrt{\tau_m}} \right) / |||\psi'\rangle||. \tag{5.91}$$

Taylor expanding the norm of the new state to second order in dW gives

$$\frac{1}{|||\psi'\rangle||} = 1 - \langle \hat{\sigma}_z \rangle^2 \frac{dt}{8\tau_m} - \frac{dt}{4\tau_m} - \frac{\langle \hat{\sigma}_z \rangle dW}{2\sqrt{\tau_m}}. \tag{5.92}$$

Multiplying out all terms and keeping to order $dW^2 = dt$ gives the increment $d\alpha = \alpha' - \alpha$ and $d\beta = \beta' - \beta$ as

$$d\alpha = -\frac{\alpha(1 - \langle \hat{\sigma}_z \rangle)^2}{8\tau_m} dt + \frac{\alpha(1 - \langle \hat{\sigma}_z \rangle)}{2\sqrt{\tau_m}} dW, \tag{5.93}$$

$$d\beta = -\frac{\beta(1 + \langle \hat{\sigma}_z \rangle)^2}{8\tau_m} dt - \frac{\beta(1 + \langle \hat{\sigma}_z \rangle)}{2\sqrt{\tau_m}} dW. \tag{5.94}$$

In the physics literature, it is common to divide both sides of this equation by dt and replace $dW/dt = \xi$ to obtain a stochastic differential equation in Itô interpretation. We can add in the dynamical terms from the standard Schrödinger equation, $i\hbar \partial_t |\psi\rangle = \hat{H}|\psi\rangle$, where $\hat{H} = (\epsilon/2)\hat{\sigma}_z + (\Delta/2)\hat{\sigma}_x$ for a more general analysis incorporating both dynamics from the measurement and dynamics from the Hamiltonian. This type of equation is called a stochastic Schrödinger equation.

https://doi.org/10.1017/9781009103909.006 Published online by Cambridge University Press

Stochastic Master Equation

If we convert the pure state dynamics into the dynamics of the density matrix (see Appendix 2 for a review of mixed quantum states), this is called a stochastic master equation. It can be derived from $\rho_{ij} = \psi_i \psi_j^*$, where no normalization is required since we already normalized the pure state dynamics. This form is more useful for experiments, because decoherence and measurement inefficiency can be incorporated, which are unavoidable in the lab. We derive the Itô form of the stochastic master equation element by element. We can express $\rho'_{00} = \alpha'^* \alpha' = (\alpha + d\alpha)^*(\alpha + d\alpha)$ and substitute the increment (5.93). Expanding to first order in dt and second order in dW, we find

$$d\rho_{00} = \rho_{00} \frac{(1 - \langle \hat{\sigma}_z \rangle)}{\sqrt{\tau_m}} dW, \tag{5.95}$$

where we replace $|\alpha|^2$ with ρ_{00} at time $t = 0$ and note $\langle \hat{\sigma}_z \rangle = \rho_{00} - \rho_{11}$. Similarly for ρ_{11}, we express $\rho'_{11} = \beta'^* \beta' = (\beta + d\beta)^*(\beta + d\beta)$, and substitute the increment (5.94). Expanding as before, we find

$$d\rho_{11} = -\rho_{11} \frac{(1 + \langle \hat{\sigma}_z \rangle)}{\sqrt{\tau_m}} dW, \tag{5.96}$$

where $|\beta|^2$ is replaced with ρ_{11}. For the off-diagonal matrix elements $\rho_{01} = \rho_{10}^*$, we have $\rho'_{01} = \alpha' \beta'^* = (\alpha + d\alpha)(\beta^* + d\beta^*)$. Substituting the increments (5.93, 5.94) and expanding to first order in dt and second order in dW, we find

$$d\rho_{01} = -\frac{\rho_{01}}{2\tau_m} dt - \frac{\rho_{01} \langle \hat{\sigma}_z \rangle}{\sqrt{\tau_m}} dW, \tag{5.97}$$

where we have replaced $\alpha\beta^*$ at $t = 0$ with ρ_{01}. We note that the sum $d\rho_{00} + d\rho_{11} = 0$, indicating that the state remains normalized, $\rho_{00} + \rho_{11} = 1$, at the end of the increment as well. Stochastic averages over the noise dW can be conveniently done in the Itô convention using property (5.82), which does not hold in other interpretations. Writing the ensemble averaged density matrix as $\bar{\rho}$, we find the equations of motion:

$$\frac{d\bar{\rho}_{00}}{dt} = \frac{d\bar{\rho}_{11}}{dt} = 0, \qquad \frac{d\bar{\rho}_{01}}{dt} = -\frac{\rho_{01}}{2\tau_m}. \tag{5.98}$$

These results indicate that the diagonal matrix elements remain at their initial values, while the coherence decays exponentially in time with rate $1/(2\tau_m)$. Thus a continuous measurement process where the results of the measurement are discarded is simply a decoherence process.

As we did before, it is convenient to express the quantum trajectory equations in the Bloch ball coordinates and include the qubit Hamiltonian

https://doi.org/10.1017/9781009103909.006 Published online by Cambridge University Press

$H = (\epsilon/2)\hat{\sigma}_z + (\Delta/2)\hat{\sigma}_x$ as well to write the final form of the Itô stochastic master equation,

$$\frac{dx}{dt} = -\frac{x}{2\tau_m} - \frac{xz}{\sqrt{\tau_m}}\xi - \epsilon y, \tag{5.99}$$

$$\frac{dy}{dt} = -\frac{y}{2\tau_m} - \frac{yz}{\sqrt{\tau_m}}\xi + \epsilon x - \Delta z, \tag{5.100}$$

$$\frac{dz}{dt} = \frac{1-z^2}{\sqrt{\tau_m}}\xi + \Delta y. \tag{5.101}$$

We stress that although these equations look different from (5.72, 5.73, 5.74) after the readout (5.75) is substituted in for r, these equations describe exactly the same physics and have the same solution once the correct interpretation of the stochastic differential equation is taken into account.

Coming back to the beginning of the analysis, we recall that the quantum state of the system remains pure during the entire process, and only by averaging over the measurement results does decoherence come into the picture. Nevertheless, in experiments, interaction with an unmonitored environment is difficult to avoid, so it is also often helpful to add in terms $-\gamma x$ or $-\gamma y$ to the first two equations to account for environmental dephasing with the rate γ. Relaxation to the ground state by spontaneous emission can be accounted for with an extra term $-\rho_{ee}/T_1$ applied to the matrix element of the excited state $|e\rangle$. Often the *efficiency* of the detector is accounted for in a similar way as described in Section 4.2. If we multiply the ensemble average decoherence rate, $d\bar{\rho}/dt = \Gamma_\phi$, by twice the measurement time (in our convention), this results in the inverse efficiency of the detector, characterizing how much information is lost to the environment,

$$\eta = \frac{1}{2\tau_m\Gamma_\phi}. \tag{5.102}$$

Here η is bounded between $0 \leq \eta \leq 1$, where an efficiency of 1 indicates no lost information, while an efficiency of 0 indicates all the information is lost. This latter case recovers the dynamics (5.98) and is equivalent to an "open quantum system," a topic we will return to soon.

This theory can now be tested against experimental practice. In Fig. 5.5, data is shown from an experiment using a superconducting quantum circuit (Murch et al., 2013b; Weber et al., 2014). Quantum trajectories are represented as expectation values of Pauli matrices, and plotted on a slice of the Bloch ball. Single trajectories may be constructed from the initial state of the qubit and data from the quantum amplifier as described in this chapter, and are plotted in the figure. By averaging over many realizations of the experiment, smooth curves (the ensemble average) are also obtained and may be compared with theory. An outstanding

https://doi.org/10.1017/9781009103909.006 Published online by Cambridge University Press

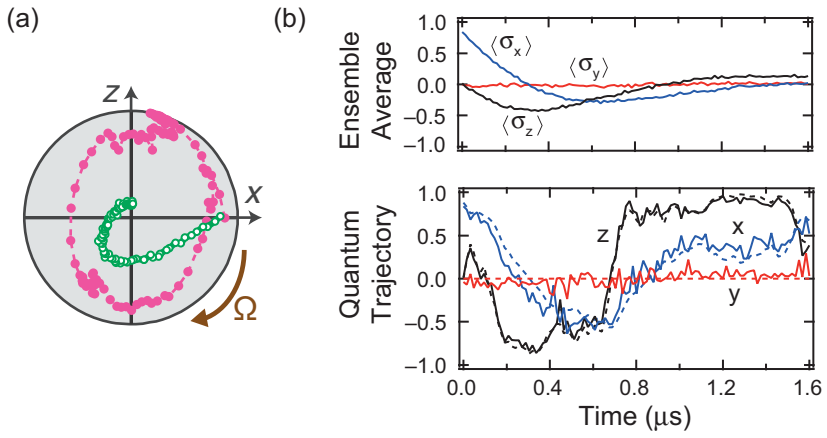

Figure 5.5 Experimental data taken of quantum trajectories with Rabi drive $\Delta = \Omega$, starting near the state $(|0\rangle + |1\rangle)/\sqrt{2}$ – repeated experimental preparation of this state is subject to slight dephasing, resulting in the experiment beginning slightly inside the Bloch ball (Murch et al., 2013b). The combination of effects coming from the Rabi drive and the continuous measurement is manifest. (a) Closed dots are data taken from a single run of the experiment. The quantum trajectory, plotted in the $x - z$ plane of the Bloch ball, is inferred from theory via the noisy output of the quantum amplifier. Open dots are the ensemble averaged quantum trajectory over many experiments, starting from the same initial state. (b) Upper panel – the ensemble averaged trajectories, represented as expectation values of the Pauli matrices are plotted versus time. Lower panel – The solid line is the quantum trajectory of a single trajectory is plotted versus time. The dashed line is the experimental tomographic reconstruction of that single trajectory, showing good agreement with theory. See the main text for a description of the tomographic procedure. Adapted with permission from Springer Nature.

question is how to experimentally validate the predictions of the theory. In panel (b) of Fig. 5.5, the following procedure was used. The experiment is allowed to proceed from the same initial state until a variable time t. At that point the continuous measurement is stopped, and the state of the qubit at that time is checked with quantum state tomography. This means a variable unitary operator is applied, followed by a conventional projective measurement, populating the readout cavity with a large number of photons, and projecting the qubit into one of its eigenstates. By repeating this procedure many times, reliable statistics can be used to validate the assigned quantum state's predictions in the different possible choices of basis. A subtlety here is that many millions of measurements must be made, because each realization of the continuous measurement process produces a different quantum state after a fixed period of time. By varying the amount of time from the beginning of the experiment until quantum state tomography measurements are performed,

https://doi.org/10.1017/9781009103909.006 Published online by Cambridge University Press

a full catalogue of the correct quantum state assignment is produced. It is then possible to validate a single quantum trajectory: each value of the quantum state at time t, along with the readout of the optical amplifier, predicts the correct state at the time time step, which can be looked up in the catalog. Those dots, when connected, can then be compared with the single trajectory quantum state assignment for each time step. The comparison, seen in panel (b), shows excellent agreement. From this experimental analysis, we conclude that it is possible to accurately make predictions of the quantum state all through the duration of a *single experiment*. Thus, while it is sometimes said that quantum mechanical predictions are only true for an ensemble of outcomes, we see here that this Bayesian point of view enables quantum state assignments even for single events that are physically powerful to predict the correct statistics of future events.

We end this subsection by pointing out that this experiment allows us to peer into the inner workings of the quantum state collapse process. It is no longer a mysterious black box to be discussed only in philosophy books, but an empirical process that can be characterized and tested extensively in the laboratory (Jordan, 2013).

5.5 Stochastic Path Integral

A powerful alternative to stochastic differential equation approaches to quantum trajectories and their statistical properties is the stochastic path integral. Just as the Feynman path integral gives a complementary understanding to quantum phenomena as well as an alternative way of calculating than the Schrödinger equation, the stochastic path integral approach does the same for the stochastic Schrödinger and master equations.

The basic idea introduced by Chantasri et al. (2013) (also called the CDJ formalism) is to calculate a master probability density of all possible measurement outcomes and associated quantum trajectories from which every possible statistical question can be answered. We return to a time-discretized description, shown in Fig. 5.6, with a time step of Δt, so there are a collection of continuous measurement results $\{r_k\}$, where $k = 1, 2, \ldots, N$, and associated quantum states $\{\hat{\rho}_k\}$, where we adopt a mixed-state picture for a fully general treatment. It is convenient to parameterize the density matrix with a set of parameters $\mathbf{q}$ that are the generalization of the Bloch coordinates. To describe higher-dimensional spaces, the Pauli matrices for a two-dimensional quantum system are expanded to a set of $n^2 - 1$ matrices in an n-dimensional system, also known as the generalized Gell-Mann matrices, appropriate for generating the group SU(n). In a two-dimensional Hilbert space, $\mathbf{q} = (x, y, z)$, the Bloch coordinates. The mapping (5.56) from one density matrix to the next time step may be expressed as $\mathbf{q}_{k+1} = \mathcal{E}(\mathbf{q}_k)$, where $\mathcal{E}$ describes

https://doi.org/10.1017/9781009103909.006 Published online by Cambridge University Press

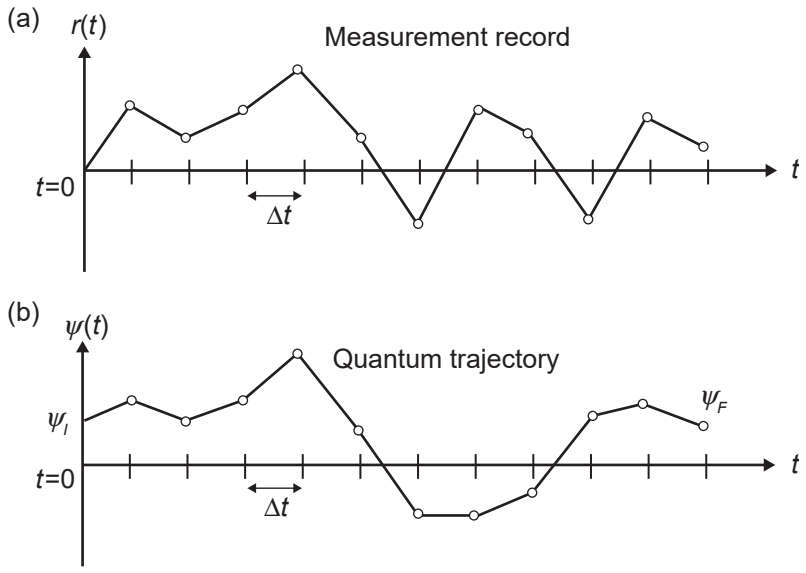

Figure 5.6 A conceptualization of the time-discredited formulation of quantum trajectory theory is shown. (a) The measurement readout $r(t)$ is plotted versus time t in time-slicing steps of Δt, taking values r_k shown in open circles. The experimental detector naturally has a finite time-resolution, given by its inverse bandwidth. (b) The corresponding quantum trajectory is schematically shown as a time-sliced function, taking values ψ_k at the open circles. Initial and final states are ψ_I and ψ_F. The progressive value of the quantum state at the next time step, ψ_{k+1}, is calculated from the current value of the state, ψ_k, and the current value of the measurement record, r_k.

the operation of the measurement operator on the parameterized density matrix (a function taking n inputs and outputting n outputs).

Let us define the master probability density of all possible measurement outcomes and associated quantum trajectories as $\mathcal{P}(\{\mathbf{q}_k\}, \{r_k\}|\mathbf{q}_i)$, starting from the initial quantum state $\mathbf{q}_i$. As is the case earlier in the chapter, we make the assumption that the time step Δt is longer than the correlation time of the noise, so the coordinates at each step depend only on the previous one (Markov approximation). In that case, we can express $\mathcal{P}$ as

$$\mathcal{P} = \prod_{k=0}^{N-1} P(\mathbf{q}_{k+1}|\mathbf{q}_k, r_k) P(r_k|\mathbf{q}_k). \tag{5.103}$$

Here, $P(r_k|\mathbf{q}_k)$ is the conditional probability distribution for r_k, given the system is in state $\mathbf{q}_k$, while $P(\mathbf{q}_{k+1}|\mathbf{q}_k, r_k)$ is the conditional probability for the new state at time step $k+1$, given result r_k is obtained. The latter is given by the update rule mentioned before, now expressed as an n-dimensional delta function,

https://doi.org/10.1017/9781009103909.006 Published online by Cambridge University Press

$$P(\mathbf{q}_{k+1}|\mathbf{q}_k, r_k) = \delta^{(n)}(\mathbf{q}_k - \mathcal{E}(\mathbf{q}_k)). \tag{5.104}$$

To make further progress, we express the delta function in Fourier form,

$$\delta(q) = \int_{-\infty}^{\infty} \frac{dp}{2\pi} e^{-iqp}, \tag{5.105}$$

and introduce a set of new variables $\mathbf{p}_k$, so the master probability takes the form

$$\mathcal{P} = \mathcal{N} \prod_{k=0}^{N-1} \int d\mathbf{p_k} \exp\left(\sum_{\mathbf{k=0}}^{\mathbf{N-1}} (-\mathbf{i}\mathbf{p_k} \cdot [\mathbf{q_k} - \mathcal{E}(\mathbf{q_k})] + \ln P(\mathbf{r_k}|\mathbf{q_k})) \right), \tag{5.106}$$

where $\mathcal{N}$ is a normalization constant. This procedure doubles the number of variables in the system. In the time-continuous limit, we replace the time index k by the time $t = k\Delta t$ and take terms in exponential to first-order in the time-step Δt, so we define

$$\mathcal{E}(\mathbf{q}_k) \approx \mathbf{q}_k + \Delta t \mathcal{L}[\mathbf{q}(t), r(t)], \qquad \ln P(r_k, \mathbf{q}_k) \approx \Delta t \mathcal{F}[\mathbf{q}(t), r(t)]. \tag{5.107}$$

Here $\mathcal{L}, \mathcal{F}$ are functionals of the coordinates.

We therefore find in the time-continuous limit the expression

$$\mathcal{P} = \int \mathcal{D}p\, e^{\mathcal{S}}, \qquad \mathcal{S} = \int_0^t dt' (-i\mathbf{p} \cdot (\dot{\mathbf{q}} - \mathcal{L}[\mathbf{q}, r]) + \mathcal{F}[\mathbf{q}, r]). \tag{5.108}$$

Here $\int \mathcal{D}p$ is a functional integral over all values of all components of $\mathbf{p}$ and absorbs any possibly divergent constants into the definition that can be found by normalization. The quantity $\mathcal{S}$ we call the *stochastic action* takes the form of a time integral over a function of the state coordinates and readouts. The action integrand has a dynamical term $-i\mathbf{p} \cdot \dot{\mathbf{q}}$, as well as a contribution we call the *stochastic Hamiltonian* in analogy to the Feynman path integral, although there is no direct connection with energy – rather we will see it plays the role of a constant of motion:

$$\mathcal{H} = i\mathbf{p} \cdot \mathcal{L}[\mathbf{q}, r] + \mathcal{F}[\mathbf{q}, r]. \tag{5.109}$$

This form of the stochastic path integral is reminiscent of the quantum description of a fictitious mechanical system with Hamiltonian $\mathcal{H}$, coordinates $\mathbf{q}$, and momentum $\mathbf{p}$. However, there are a number of differences. Since this action describes diffusive motion, the action can be made real, after rotating the contour of the p integrals along the imaginary axis. The dimension of the fictitious mechanical system is the same as the Hilbert space of the system. Further, while Feynman paths are taken through configuration space, it is essential to note here the paths of the path integral are through the Hilbert space of the quantum system (more generally the quantum state space). The interpretation of the momentum-like variables $\mathbf{p}$ is analogous to momentum in the sense that they generate translations of the canonically conjugate coordinates $\mathbf{q}$, which do have a direct physical meaning. Further,

https://doi.org/10.1017/9781009103909.006 Published online by Cambridge University Press

the theory has a canonical structure, so changes of variables of the $\mathbf{q}$ coordinates must be accompanied by changes of $\mathbf{p}$ coordinates that are canonically invariant – that is, the Poisson brackets must be preserved. Physically, the stochastic Hamiltonian $\mathcal{H}$ encodes the detailed physics of the quantum measurement process – the nature of the probability distribution of the results, as well as the form of quantum backaction that is appropriate to the kind of measurement one is making. If the kind of measurement that is being carried out changes, the form of the stochastic action will also change, just like the right-hand side of the stochastic Schrödinger or master equation will change.

From the master probability distribution function $\mathcal{P}$, various quantities can be calculated, such as correlation functions of the form

$$\langle A(x_1, x_2, \ldots x_M)\rangle = \int \mathcal{D}q\mathcal{D}q\mathcal{D}rA(x_1, x_2, \ldots x_M)e^{\mathcal{S}}, \tag{5.110}$$

where the x variables represent any function of $\mathbf{q}$ or r at times $t_1, t_2, \ldots, t_M$. More generally, we can also account for additional constraints of a conditional nature. For example, if we also wish to impose a final boundary condition, this can done by only allowing quantum trajectories in the averages that end at a desired end point $\mathbf{q}_f$. In future chapters, we will explore a natural application of this formalism that is completely hidden in the stochastic differential equation approach: the concept of the most likely path the quantum system takes between final and initial conditions. The most likely path is analogous to the emergence of the classical path from the Feynman path integral in the limit of small $\hbar$, which gives rise to a new kind of action principle for a continuously measured quantum system.

We now give a few example applications of this formalism.

Application to the Case of Continuous Dispersive Qubit Measurement

Let us return to the continuously measured qubit example explored earlier in this chapter. The ingredients we need are the qubit coordinates – here simply the Bloch coordinates used in Eqs. (5.72, 5.73, 5.74), as well as the functionals $\mathcal{L}, \mathcal{F}$. The associated pseudo-momenta we call p_x, p_y, p_z and are canonically conjugate to x, y, z. To find $\mathcal{F}$, we recall that the distribution of result r is given by Eq. (5.55). Expanding the logarithm of $P(r|\mathbf{q})$ to first order in Δt, we find

$$\ln P(r|\mathbf{q}) \approx -\frac{\Delta t}{2\tau_m}(r^2 - 2rz + 1), \tag{5.111}$$

where we drop higher-order terms in Δt and absorb the constant term of order $\ln \Delta t$ into the normalization of the path integral. Consequently, $\mathcal{F} = (-r^2 + 2rz - 1)/(2\tau_m)$. To find $\mathcal{L}$, we make the expansion of the state disturbance equation to first order in Δt and find Eqs. (5.72, 5.73, 5.74). We can also add in dephasing from an

https://doi.org/10.1017/9781009103909.006 Published online by Cambridge University Press

unmonitored environment (which is equivalent to loss or inefficient measurement) by putting in additional decay terms of the form $-\gamma(x,y)$ for the coherence equations of motion. Putting all this together, we find the stochastic action to be given by

$$\mathcal{S} = \int_0^t dt'[-ip_x(\dot{x} + \gamma x + \epsilon y + xzr/\tau_m) - ip_y(\dot{y} + \gamma y - \epsilon x + \Delta z + yzr/\tau_m) - ip_z(\dot{z} - \Delta y - (1-z^2)r/\tau_m) - (r^2 - 2rz + 1)/(2\tau_m)]. \tag{5.112}$$

From this form of the action, any statistical quantity of interest can now be calculated in principle.

5.6 Diffusive Measurement with Continuous Variables

In the example just given, we focused on a finite-dimensional system to illustrate the formalism and main results. However, in quantum physics we are often interested in continuous systems, such as a particle bound in a potential well, or in a scattering problem. The stochastic path integral approach has recently been applied to Gaussian state evolution in a harmonic potential undergoing joint position and momentum measurement (Karmakar et al., 2022). How continuous measurements of such systems can be described in a more general context will complete this chapter on diffusive continuous measurement.

Let us make a connection also with the Feynman path integral by considering the quantum description of a continuous measurement of the position of a particle of mass m in a potential well $V(x)$. We consider a meter that weakly measures the position operator $\hat{x}$ of the particle, repeatedly at intervals of time Δt. The measurement operator is taken to be

$$\hat{\Omega}_k = \left(\frac{\pi\sigma^2}{\Delta t}\right)^{1/4} \exp\left[-\frac{\Delta t}{4\sigma^2}(r_k - \hat{x})^2\right]. \tag{5.113}$$

Here, r_k is the measurement result at time interval k. We can find the probability density of result r_k by using the results from Chapter 3, assuming that at the previous time, the quantum wavefunction of the particle is given by $\psi_k(x)$. This yields

$$P(r_k|\psi_k) = \int_{-\infty}^{\infty} dx|\psi_k(x)|^2 \sqrt{\frac{\pi\sigma^2}{\Delta t}} \exp\left(-\frac{\Delta t}{2\sigma^2}(r_k - x)^2\right). \tag{5.114}$$

The mean of this distribution is given by $\langle\psi_k|\hat{x}|\psi_k\rangle$. The variance is given by $\mathrm{Var}[r_k] = \sigma^2/\Delta t + \mathrm{Var}[\hat{x}]$, where the variance of $\hat{x}$ is with respect to the state $|\psi_k\rangle$. In the limit where Δt is small, the weak measurement limit, the variance

https://doi.org/10.1017/9781009103909.006 Published online by Cambridge University Press

associated with the imprecise measurement, $\sigma^2/\Delta t$, is much larger than the position variance of the wavefunction, so the latter may be neglected. In this limit, we can treat the squared wavefunction like a delta function under the integral, centered at the expectation value of the position operator, with respect to the wavefunction, so the probability distribution may be well approximated as

$$P(r_k|\psi_k) \approx \sqrt{\frac{\pi\sigma^2}{\Delta t}} \exp\left(-\frac{\Delta t}{2\sigma^2}(r_k - \langle x\rangle_k)^2\right), \tag{5.115}$$

where $\langle x\rangle_k = \langle\psi_k|\hat{x}|\psi_k\rangle$.

The new wavefunction $\psi_{k+1}(x)$ is given by

$$\langle x|\psi_{k+1}\rangle = \frac{\langle x|\hat{U}_k\hat{\Omega}_k|\psi_k\rangle}{\sqrt{P(r_k|\psi_k)}}. \tag{5.116}$$

Here we have added in the unitary dynamics described by the Hamiltonian $H = \hat{p}^2/(2m) + V(\hat{x})$ as $\hat{U}_k = \exp(-i\Delta t\hat{H}_k/\hbar)$. The operator ordering of $\hat{U}$ and $\hat{\Omega}$ does not matter since the commutator is of order Δt^2. Inserting a complete set of position and momentum states, we find

$$\begin{aligned}\psi_{k+1}(x_{k+1}) = \int \frac{dx_k dp_k}{2\pi\hbar} \exp[ip_k(x_{k+1} - x_k)/\hbar - i\frac{p_k^2\Delta t}{2m\hbar} - i\frac{V(x_k)\Delta t}{\hbar} \\ - \frac{\Delta t}{4\sigma^2}(x_k - \langle x\rangle_k)^2 + \frac{\Delta t}{2\sigma^2}r_k(x_k - \langle x\rangle_k)]\psi_k(x_k).\end{aligned} \tag{5.117}$$

This process can be repeated to generate the final state $\psi_N(x_N)$, given by a generalized propagator,

$$\psi(x', t) = \int dx\mathcal{M}(x', x, t)\psi(x, 0), \tag{5.118}$$

where the generalized propagator is given by

$$\mathcal{M}(x', x, t) = \int \mathcal{D}x\mathcal{D}p e^{\mathcal{S}}, \tag{5.119}$$

$$\mathcal{S} = \int_0^t dt' \left[\frac{i}{\hbar}(p\dot{x} - \frac{p^2}{2m} - V(x)) - \frac{x^2 - \langle x\rangle^2}{4\sigma^2} + \frac{r(x - \langle x\rangle)}{2\sigma^2}\right].$$

Here the boundary conditions are $x(0) = x$ and $x(t) = x'$ and $\mathcal{D}x\mathcal{D}p = \prod_k \frac{dx_k dp_k}{2\pi\hbar}$. The function $\langle x\rangle(t)$ is the time-local expectation value of position, given the state at that time. The function $r(t)$ is the stochastic readout, which is a random time-continuous variable drawn from the distribution

$$P[r(t)] = \mathcal{N} \exp\left(-\int_0^t \frac{dt}{2\sigma^2}(r - \langle x\rangle)^2\right), \tag{5.120}$$

https://doi.org/10.1017/9781009103909.006 Published online by Cambridge University Press

where $\mathcal{N}$ is a normalization constant. That is, the variable r is a Gaussian random variable, with mean $\langle x \rangle$ at that time. It can be expressed as

$$r(t) = \langle x \rangle(t) + \sigma\, \xi, \tag{5.121}$$

where ξ is a delta-correlated random variable with strength 1. Indeed, we can eliminate the readout variable r from the system discussion and reexpress the stochastic action for the system as

$$\tilde{\mathcal{S}} = \int_0^t dt' \left[\frac{i}{\hbar}(p\dot{x} - \frac{p^2}{2m} - V(x)) - \frac{(x - \langle x \rangle)^2}{4\sigma^2} + \frac{(x - \langle x \rangle)\xi}{2\sigma} \right]. \tag{5.122}$$

This result may be interpreted as the usual Feynman path integral in Hamiltonian form, but with two additions. The first (Gaussian) term provides a (real) contribution to the action that suppresses paths that wander more than a distance σ from the mean value of the position. The feature is reminiscent of Mensky's "restricted path integral," where corridors to restrict the particle's motion are put in by hand in order to rule out paths forbidden by the measurement results (Mensky, 1994). The second additional term to the action is also real but can be interpreted as a stochastic force causing the particle's position to be randomly kicked as the result of the measurement. These results are related to those of Caves and Milburn (1987). We will explore this interpretation more in the analysis of the most likely path.

While the time-continuous integrals provide an elegant representation, when going to a stochastic differential equation, confusion can arise. The corresponding stochastic differential equation to the update rule (5.116) can be derived by expanding to first order in the time-step to find

$$\frac{d|\psi\rangle}{dt} = \left[-i\hat{H}/\hbar + \frac{r}{2\sigma^2}(\hat{x} - \langle x \rangle) - \frac{1}{4\sigma^2}(\hat{x}^2 - \langle x \rangle^2) \right] |\psi\rangle. \tag{5.123}$$

Here, if we replace $r(t)$ by the signal and noise decomposition (5.121), where $\xi = dW/dt$, we obtain

$$\frac{d|\psi\rangle}{dt} = \left[-i\hat{H}/\hbar + \frac{\xi}{2\sigma}(\hat{x} - \langle x \rangle) - \frac{1}{4\sigma^2}(\hat{x} - \langle x \rangle)^2 \right] |\psi\rangle. \tag{5.124}$$

Here, $\langle x \rangle = \langle \psi | \hat{x} | \psi \rangle$ at time t. We must interpret the preceding stochastic differential equation in the Stratonovich sense. The deeper reason for this is that the equation is derived from physical considerations, therefore the stochastic noise function ξ obtained by subtracting the expected position from the measured signal can never be perfect white noise. This goes back to the previous discussion, where we insisted upon the separation of timescales between the correlation time of the noise and the dynamical timescales of the system of interest. In reality, every such physical approximation to white noise has more regular properties. In two

https://doi.org/10.1017/9781009103909.006 Published online by Cambridge University Press

important papers, Wong and Zakai proved that the solution to the *ordinary differential equation*, which is obtained from the stochastic differential equation by replacing the noise term with a continuous approximation to the Brownian motion, converges to that of the Stratonovich stochastic differential equation in the limit where the approximated Brownian motion becomes better and better (Wong and Zakai, 1965a,b). Thus, while the stochastic path integral is perfectly well defined as we constructed it, the corresponding differential equations need their proper interpretation. For completeness, the Itô form of the stochastic differential equation is found by expanding (5.116) to second order in $\xi = dW/dt$ and using Itô's rule as discussed earlier in this chapter to find

$$\frac{d|\psi\rangle}{dt} = \left[-i\hat{H}/\hbar + \frac{\xi}{2\sigma}(\hat{x} - \langle x\rangle) - \frac{1}{8\sigma^2}(\hat{x} - \langle x\rangle)^2\right]|\psi\rangle. \tag{5.125}$$

where the coefficient of the drift term is changed.

Exercises

Exercise 5.6.1 Prove that the states $|\psi_\pm\rangle = (|L\rangle \pm |R\rangle)/\sqrt{2}$ describe the ground and first excited states of the DQD, respectively. Use two different methods:
(i) In the spatially symmetric case, the states should have definite parity, so under exchange of $L \leftrightarrow R$, the eigenstates are invariant up to an overall sign. Show that the $\langle x|\psi_+\rangle$ wavefunction has no nodes and must therefore be the ground state, while the $\langle x|\psi_-\rangle$ wavefunction has one node and must therefore be the first excited state.
(ii) If an electron tunnels from the left to the right well with rate $\Delta/\hbar$, we can model an effective two-state system with a Hamiltonian $\hat{H} = \Delta\hat{\sigma}_x$ in the left/right basis. Therefore $|\psi_\pm\rangle$ diagonalizes the effective Hamiltonian.

Exercise 5.6.2 Prove Eq. (5.2) is correct by solving the time-dependent Schrödinger equation.

Exercise 5.6.3 Work out the case described in Section 5.3.1, where the qubit state is mixed, and show that if we average over both outcomes, the degree of decoherence is $C_{LR} = t_L t_R^* + r_L r_R^*$, which has norm less than 1.

Exercise 5.6.4 Show that starting from Eq. (5.22), the dispersive form of the Jaynes–Cummings Hamiltonian (5.25) can be found by making use of the unitary transformation

$$\hat{U} = \exp[(g/\Delta)(\hat{a}^\dagger\hat{\sigma}_- - \hat{a}\hat{\sigma}_+)], \tag{5.126}$$

on the original Hamiltonian, and expanding to second order in g/Δ.

Exercise 5.6.5 Consider the case of monitored spontaneous emission of a two-level atom. Consider a single field mode with no photons, $|0\rangle$, and the two-level atom prepared in the state $\phi|g\rangle + \zeta|e\rangle$, where $|e\rangle, |g\rangle$ are the excited

https://doi.org/10.1017/9781009103909.006 Published online by Cambridge University Press

and ground states of the atom, and ϕ, ζ are complex amplitudes. After a short time δt, the atom can decay to the ground state and emit a photon with a rate γ, so the emission probability is $\epsilon = \gamma \delta t$. Show that the state at time δt is given by

$$|\psi\rangle = \sqrt{1-\epsilon}\zeta|e,0\rangle + \sqrt{\epsilon}\zeta|g,1\rangle + \phi|g,0\rangle, \tag{5.127}$$

where $|1\rangle$ denotes a single photon emitted into the field mode. See Jordan et al. (2016) for further discussion.

Exercise 5.6.6 Suppose the field mode is detected with a homodyne detection scheme, described by projection of the field mode state onto the operator $\hat{X} = (\hat{a} + \hat{a}^\dagger)/\sqrt{2}$, where $\hat{a}$ and $\hat{a}^\dagger$ are the creation and annihilation operators of the optical field. Let $|X\rangle$ be the eigenstate of this operator. Show

$$\langle X|0\rangle = \pi^{-1/4} e^{-X^2/2}, \quad \langle X|1\rangle = \pi^{-1/4}\sqrt{2}Xe^{-X^2/2}. \tag{5.128}$$

Exercise 5.6.7 Combine the previous two exercises to show that the measurement operator for amplifying the spontaneous emission of the homodyne detection is given by

$$\hat{M}_X = e^{-X^2/2}\begin{pmatrix}\sqrt{1-\epsilon} & 0\\ \sqrt{2\epsilon}X & 1\end{pmatrix}, \tag{5.129}$$

where X is the outcome of the quadrature measurement. Hint: Make an analogy to the quantum harmonic oscillator.

Exercise 5.6.8 Scaling the readout $X \to \sqrt{dt/2}r$ in the previous problem, show that the random variable r has a mean $\sqrt{\gamma}x$, and variance $1/dt$.

Exercise 5.6.9 For the scaling of X in the previous problem, show that the analogous equations of motion to Eqs. (5.72, 5.73, 5.74) are given by

$$\dot{x} = \frac{\gamma}{2}xz + \sqrt{\gamma}r(1+z-x^2) - \epsilon y, \tag{5.130}$$

$$\dot{y} = \frac{\gamma}{2}yz - \sqrt{\gamma}rxy + \epsilon x - \Delta z, \tag{5.131}$$

$$\dot{z} = \frac{\gamma}{2}(z^2-1) - \sqrt{\gamma}r(1+z)x + \Delta y. \tag{5.132}$$

https://doi.org/10.1017/9781009103909.006 Published online by Cambridge University Press